Electronic Supplementary Material (ESI) for Chemical Science.
This journal is © The Royal Society of Chemistry 2023

Electronic Supplementary Information
for

Rational Design and Topochemical Synthesis of Polymorphs of a Polymer

Vignesh Athiyarath,[a] Liby Ann Mathew,[a] Yakai Zhao,[b] Ravichandran Khazeber,[a] Upadrasta Ramamurty,[b] and Kana M. Sureshan*[a]

[a]School of Chemistry, Indian Institute of Science Education and Research Thiruvananthapuram, Kerala-695551 (India).
[b]School of Mechanical and Aerospace Engineering, Nanyang Technological University, Singapore-639798.

*Kana M. Sureshan, **Email:** kms@iisertvm.ac.in

This PDF file includes:

Section S1. Materials and methods

All the chemicals and solvents were purchased from various commercial sources and were used without further purification. Pre-coated TLC silica gel 60 F254 plates were purchased from Merck. TLC chromatograms were visualized under UV light and further by heating the plates after dipping them in ceric ammonium molybdate staining solution. Silica gel (230-400 mesh) used for column chromatography was purchased from Finar Limited. NMR spectra of compounds dissolved either in deuterated chloroform or dimethyl sulfoxide were recorded on Avance III-500 (Bruker) NMR spectrometer. The chemical shifts δ were reported in ppm relative to tetramethylsilane (TMS). IR spectra were recorded using IR Prestige-21 (Shimadzu) spectrometer. Elemental analyses were done on Elementar, vario MICRO cube elemental analyzer. Powder X-ray diffraction (PXRD) spectra were recorded using an X'pert PRO (PANalytics) powder diffractometer with Cu as the anode material (Kα1 = 1.540598 Å). Single Crystal X-Ray Diffraction (SCXRD) data measurements were carried on a Bruker-KAPPA APEX II CCD diffractometer with graphite-monochromatized (MoK = 0.71073 Å) radiation. The X-ray generator was operated at 50 kV and 30 mA. The X-ray data collection was analyzed by SMART program (Bruker, version 5.631, 2004). All the data were corrected for Lorentzian polarization and absorption effects using SAINTPLUS and SADABS programs (Bruker, 2004).[1,2] SHELXT and SHELXL-2014 were used for structure solution and full matrix least-squares refinement on F2.[3,4] Analysis of the crystal structure was done using the Mercury 3.9 software.[5] Face indexing of single crystals was carried out using Bruker AXS Face-indexing User Interface, from a Bruker KAPPA APEX-II diffractometer in omega and phi scan mode. TGA profile of the polymers was recorded using Universal V4.7A TA instrument at a heating rate of 5 °C/min. Gel Permeation Chromatography (GPC) is performed using Agilent 1260 Infinity II GPC/SEC System using a solution of 0.1 % LiBr in DMF as eluent.

Section S2. Synthesis of tripeptide 1

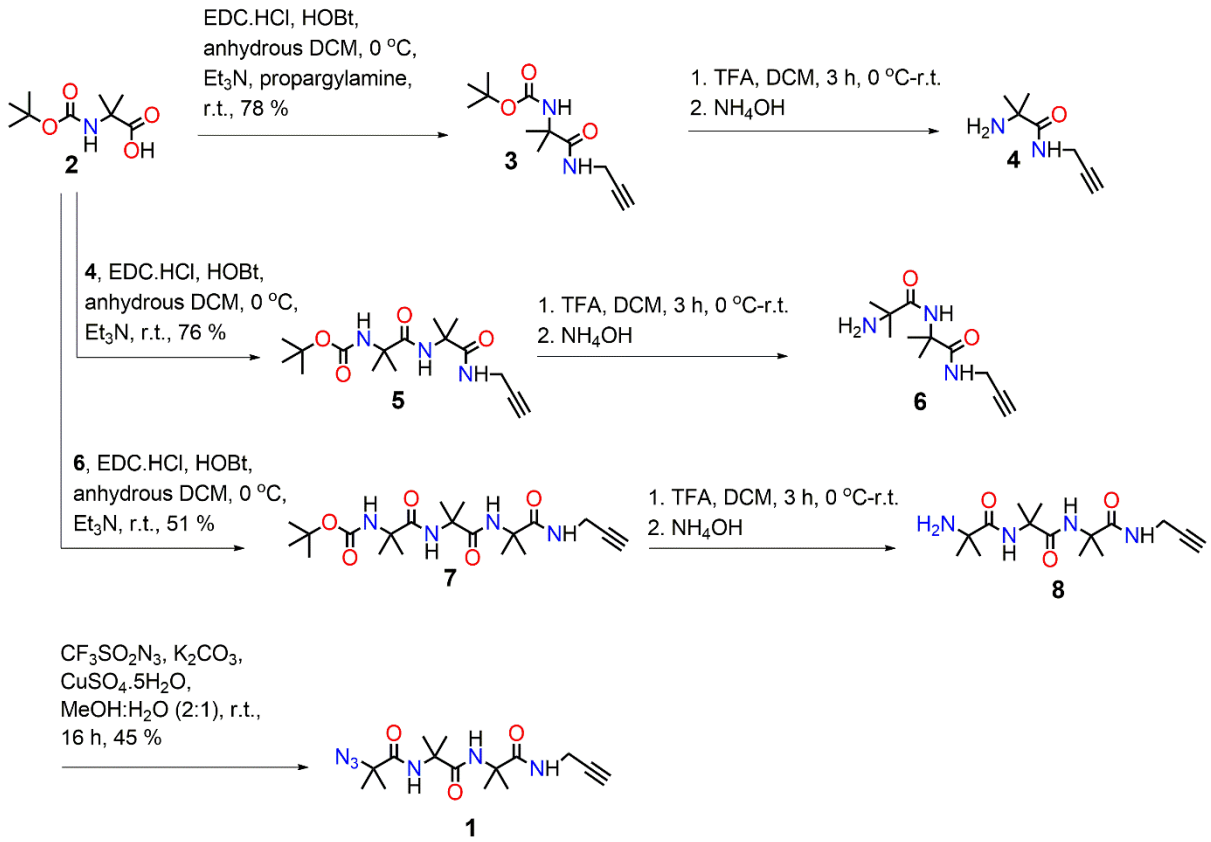

Scheme S1. Synthesis of tripeptide **1**

a) <u>Procedure A</u>: General procedure used for coupling a carboxylic acid with an amine

To a cooled (0 °C) solution of acid (1 eq.) in anhydrous DCM, EDC.HCl (1.1 eq.) and then HOBt (1.1 eq.) were added. The reaction mixture was stirred at 0 °C for 15-20 minutes. A solution of amine (1 eq.) in DCM and Et_3N (2 eq.) were added successively. The reaction mixture was stirred at room temperature for 16 h was transferred into a separating funnel. The organic layer was washed with ice-cooled 5 % HCl twice followed by saturated $NaHCO_3$ solution, water and then brine. The organic layer was dried over anhydrous Na_2SO_4 and concentrated under reduced pressure.

b) <u>Procedure B</u>: General procedure used for deprotection of Boc

To a solution of Boc protected derivative (1 eq.) in DCM at 0 °C, TFA was added (10 eq.) and the reaction mixture was stirred at room temperature for 2 hrs. At complete consumption of starting material, as shown by the TLC, the solvents were evaporated under reduced pressure. The residue was co-evaporated with anhydrous toluene. The residue was diluted with water and cooled to 0 °C. A 25 % solution of NH_4OH was added dropwise until the solution is basic (pH ≃ 10) as shown by a pH paper. The resulting solution was extracted using EtOAc. The solvent was removed under reduced pressure to obtain amine and was used for the next reaction without further purification.

c) Synthesis of Boc-Aib-propargylamide (3)

Procedure A was followed using Boc-Aib **4** (12 g, 59 mmol), propargylamine (3.78 mL, 59 mmol), EDC.HCl (12.5 g, 65 mmol), HOBt (8.81 g, 65 mmol) and Et_3N (16 mL, 118 mmol). Column chromatography was performed using a mixture of EtOAc: petroleum ether (3:7, v/v) as eluent to obtain the propargylamide **3** (11 g) in 78 % yield as a colorless powder. Melting point = 107-108 °C. R_f = 0.3 (EtOAc: petroleum ether, 3:7, v/v). ^{1}H NMR (500 MHz, DMSO-d_6) δ (ppm); 7.89 (s, 1H, -NH), 6.78 (s, 1H, -NH), 3.81 (dd, J = 5.6 Hz, J = 2.5 Hz, 2H, -CH_2), 3.01 (t, J = 2.45 Hz, 1H, -C≡CH), 1.38 (s, 9H, -C(CH_3)$_3$), 1.29 (s, 6H, -CH_3). ^{13}C NMR (125 MHz, DMSO-d_6) δ (ppm): 174.7 (CO), 154.68 (CO), 81.99 (-C≡CH), 78.44 (-C(CH$_3$)$_3$), 72.83 (-C≡CH), 56.11 (-

C(CH_3)$_2$), 28.85 (-*C*H_2), 28.64 ((-C(*C*H_3)$_3$), 25.56 (-C(*C*H_3)$_2$); Elemental analysis calculated for $C_{12}H_{20}N_2O_3$: C, 59.98; H, 8.39; N, 11.66; Found: C,60.15; H,8.53; N,11.99.

d) Synthesis of Boc-(Aib)$_2$-propargylamide (5)

The propargylamide **3** (8 g, 0.033 mol) was subjected to procedure B (using 25.7 mL TFA (0.33 mol). The amine **4** thus obtained was used in procedure A along with Boc-Aib (6.76 g, 33 mmol), EDC.HCl (6.9 g, 36 mmol), HOBt (4.86 g, 36 mmol) and Et_3N (10 mL, 72 mmol). The residue obtained was purified using column chromatography using EtOAc: petroleum ether (7:3, v/v) to obtain Boc-(Aib)$_2$-propargylamide **5** (8.2 g) in 76 % yield as a colorless powder. Melting point = 166 -167 ^oC. R_f = 0.35 (EtOAc: petroleum ether, 1:4, v/v). ^1H NMR (500 MHz, DMSO-d$_6$) δ (ppm): 7.84 (s, 1H, -NH), 7.59 (s, 1H, -NH), 7.22 (s, 1H, -NH), 3.82 (dd, *J* = 5.33 Hz, 2.3 Hz, 2H, -C*H*$_2$), 3.03 (s, 1H, -C≡C*H*), 1.42 (s, 9H, -C(C*H*$_3$)$_3$),1.33 (s, 6H, -C(C*H*$_3$)$_2$), 1.26 (s, 6H, -C(C*H*$_3$)$_2$). ^{13}C NMR (125 MHz, DMSO-d$_6$) δ (ppm): 174.77 (CO), 174.02 (CO) 155.74 (CO), 81.36 (-*C*≡CH), 79.25 (-*C*(CH$_3$)$_3$), 73.23 (-C≡*C*H), 56.35 (-*C*(CH$_3$)$_2$, 56.23 (-*C*(CH$_3$)$_2$), 28.89 (-*C*H$_2$), 28.71, (-*C*(CH$_3$)$_3$), 25.32 (-C(CH$_3$)$_2$); Elemental analysis calculated for $C_{16}H_{27}N_3O_4$: C, 59.06; H, 8.36; N, 12.91; Found: C, 58.43; H, 8.47; N,12.7.

e) Synthesis of Boc-(Aib)$_3$-propargylamide (7)

Compound **5** (8 g, 25 mmol) was subjected to procedure B (using 18.9 mL TFA) and the amine **6** thus obtained was subjected to procedure A along with Boc-Aib (5 g, 25 mmol), EDC.HCl (5.19 g, 27 mmol), HOBt (3.65 g, 27 mmol) and Et_3N (7.5 mL, 54 mmol). The residue obtained was purified using column chromatography using a mixture of EtOAc: petroleum ether (7:3, v/v) to obtain Boc-(Aib)$_3$-propargylamide **7** (5.1 g) in 51 % yield as a colorless powder. Melting point = 225 - 226 ^oC. R_f = 0.3 (EtOAc: petroleum ether, 7:3, v/v). ^1H NMR (500 MHz, DMSO-d$_6$) δ (ppm); 8.15 (s, 1H, -NH), 7.75 (t, *J* = 5.4 Hz, 1H, -NH), 3.82 (dd, *J* = 5.45 Hz, *J* = 2.45 Hz, 2H, -CH$_2$), 3.0 (t, *J* = 2.45 Hz, 1H, -C≡C*H*), 1.43 (s, 9H, -C(C*H*$_3$)$_3$), 1.36 (s, 6H, -C(CH$_3$)$_2$), 1.3 (s, 6H, -C(CH$_3$)$_2$), 1.27 (s, 6H, -C(CH$_3$)$_2$). ^{13}C NMR (125 MHz, DMSO-d$_6$) δ (ppm):175.72 (CO), 174.75 (CO), 173.91 (CO), 155.8 (CO), 81.47 (-*C*≡CH), 79.41 (-*C*(CH$_3$)$_3$, 72.95 ((-C≡*C*H), 56.49 (-*C*(CH$_3$)$_2$), 56.46 (-*C*(CH$_3$)$_2$), 56.27 (-*C*(CH$_3$)$_2$), 28.83 (-*C*H$_2$), 28.59 (-C(*C*H$_3$)$_3$), 25.81 (-C(*C*H$_3$)$_2$), 25.31 (-C(*C*H$_3$)$_2$), 25.06 (-C(CH$_3$)$_2$); Elemental analysis calculated for $C_{20}H_{34}N_4O_5$: C, 58.52; H, 8.35; N, 13.65; Found: C, 58.85; H, 8.01; N, 13.8.

f) Synthesis of tripeptide 1

***Preparation of triflyl azide*:** NaN_3 (8 g, 0.12 mol) was dissolved in a 400 mL mixture of DCM: water (1:1, v/v) and cooled to 0 ^oC. Triflic anhydride (4.1 mL, 0.024 mol) was added through an additional funnel dropwise over 15 minutes. The reaction mixture was stirred at room temperature for 3 hours and the contents were transferred to a separating funnel. DCM layer was collected and the aqueous layer was extracted with DCM (2 x 30 mL). The combined DCM fractions were washed once with saturated Na_2CO_3 solution (100 mL)

The propargylamide **7** (5 g, 12 mmol) was subjected to procedure B (using 9.4 mL TFA) to obtain corresponding amine **8**. $CuSO_4.5H_2O$ (30 mg, 0.12 mmol) and K_2CO_3 (2.5 g, 18 mmol) were dissolved in a 400 mL mixture of water: methanol (3:5, v/v) and amine **8** was added to it, followed by a solution of triflyl azide in DCM obtained previously. Methanol was added till the solution becomes clear and the reaction mixture was stirred at room temperature for 16 h. The solvents were evaporated under reduced pressure and the residue was dissolved in EtOAc (100 mL). The organic layer was washed with water (3 x 25 mL), dried over anhydrous Na_2SO_4, and concentrated under reduced pressure. The residue obtained was purified by column chromatography using EtOAc/petroleum ether as eluent (3:2, v/v) to obtain tripeptide **1** (1.7 g) in 45 % yield the tripeptide **1** as a colorless powder. ^1H NMR (500 MHz, DMSO-d$_6$) δ (ppm); 7.89 (s, 1H, -NH), 7.71 (t, 1H, *J* = 5.2 Hz, 1H, -NH), 7.49 (s, 1H, -NH), 3.8 (dd, *J* = 5.3 Hz, *J* = 2.25 Hz, 2H, -C*H*$_2$), 3.03 (t, *J* = 2.1 Hz, 1H, -C≡C*H*), 1.46 (s, 6H, -C(CH$_3$)$_2$), 1.36 (s, 6H, -C(CH$_3$)$_2$), 1.34 (s, 6H, -C(CH$_3$)$_2$). ^{13}C NMR (125 MHz, DMSO-d$_6$) δ (ppm): 174.56 (CO), 173.24 (CO), 172.38 (CO), 81.51 (-*C*≡CH), 73.11 (-C≡*C*H), 64.21 (-*C*(CH$_3$)$_3$), 56.94 ((-*C*(CH$_3$)$_3$), 56.39 (-*C*(CH$_3$)$_3$), 28.89 (-*C*H$_2$), 25.26 (-CH$_3$), 24.83 (-CH$_3$), 24.42 (-CH$_3$). Elemental analysis calculated for $C_{15}H_{24}N_6O_3$: C, 53.56; H, 7.19; N, 24.98; Found: C, 53.24; H, 7.236; N, 25.19.

Section S3. Crystal structure data of tripeptide 1

3a. Crystal structure data for polymorph I of tripeptide 1

Table S1:

CCDC No.	2208399	
Empirical formula	$C_{15}H_{24}N_6O_3$	
Formula weight	336.39	
Temperature (K)	296(2)	
Wavelength (Å)	0.71073	
Crystal system	Monoclinic	
Space group	$P2_1/c$	
Unit cell dimensions	a = 18.146(4) Å	α = 90.00(3)°
	b = 10.719(2) Å	β = 94.90(3)°
	c = 18.540(4) Å	γ = 90.00(3)°
Volume ($Å^3$)	3593.0(13)	
Z	8	
Calculated density (g/cm^3)	1.244	
Absorption coefficient (mm^{-1})	0.090	
F(000)	1440	
Crystal size (mm^3)	0.210 x 0.120 x 0.085	
Theta range for data collection	2.197° to 25.000°	
Index ranges	-21<=h<=21, -12<=k<=12, -22<=l<=22	
Reflections collected	47089	
Independent reflections	6317 [R(int) = 0.0712]	
Completeness to theta = 25.242°	100.0 %	
Absorption correction	Semi-empirical from equivalents	
Max. and min. transmission	0.992 and 0.981	
Refinement method	Full-matrix least-squares on F2	
Data / restraints / parameters	6317 / 0 / 433	
Goodness-of-fit on F^2	1.032	
Final R indices [I>2sigma(I)]	R1 = 0.0525, wR2 = 0.1133	
R indices (all data)	R1 = 0.1039, wR2 = 0.1385	
Extinction coefficient	n/a	
Largest diff. peak and hole ($e.Å^{-3}$)	0.184 and -0.267	

3b. ORTEP diagram of polymorph I of tripeptide 1

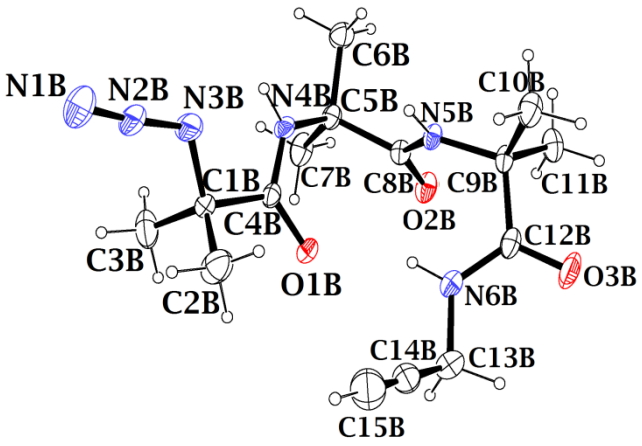

Fig. S1. ORTEP diagram of polymorph **I** of tripeptide **1** drawn with 50 % probability of ellipsoids.

3c. Non-covalent interactions present in polymorphs I

Table S2:

Type of interaction	D-H···A or N···O	Distance (H...A) (Å)
N-H···O	N5A-H5A···O3B	2.098
	N5B-H5B···O3A	2.271
	N4B-H4B···O2B	2.727
	N4A-H4A···O2A	2.639
C-H···N	C13A-H13A···N1A	2.784
	C13B-H13D···N1B	2.803
	C6B-H6B1···N3B	2.837
C-H···O	C6A-H6A3···O2A	2.777
	C7A-H7A2···O2A	2.770
	C10A-H10B···O3B	2.744
	C6A-H6B2···O2B	2.738
	C10A-H10C···.O3B	2.757
	C7A-H7B3···O2B	2.818
	C10B-H10E···O3A	2.429
C-H···H-C	C11A-H11B···H3A3-C3A	2.470
	C6A-H6A2···H10D-C10B	2.453
	C11A-H11C···H15B-C15B	2.476
	C15A-H15A···H10F-C10B	2.388
C-H···C	C6A-H6A2···C10B	2.919
	C10A-H10A···C6B	2.944
	C2B-H2B3···C14A	2.962
	C10B-H10E···C6A	2.884
	C11A-H11A···C15A	2.891
	C2B-H2B3···C14A	2.962

3d. Crystal structure data for polymorph II of tripeptide 1 determined at 150 K and 296 K

Table S3:

CCDC No.	2208396		2247295	
Empirical formula	$C_{15}H_{24}N_6O_3$		$C_{15}H_{24}N_6O_3$	
Formula weight	336.40		336.40	
Temperature (K)	150(2)		296(2)	
Wavelength (Å)	0.71073		0.71073	
Crystal system	Orthorhombic		Orthorhombic	
Space group	*Pna*2$_1$		*Pna*2$_1$	
Unit cell dimensions	a = 11.153(3) Å	α = 90°	a = 11.2274(13) Å	α = 90°
	b = 9.171(3) Å	β = 90°	b = 9.2607(12) Å	β = 90°
	c = 18.019(6) Å	γ = 90°	c = 18.166(2)	γ = 90°
Volume Å^3	1843.1(10)		1888.8(4)	
Z	4		4	
Density (calculated) g/cm^3	1.212		1.183	
Absorption coefficient (mm^{-1})	0.087		0.085	
F(000)	720		720	
Crystal size (mm^3)	0.120 x 0.095 x 0.055		0.098 x 0.068 x 0.048 mm	
Theta range for data collection	2.261° to 24.999°		2.242° to 28.384°	
Index ranges	-13<=h<=12, -10<=k<=10, -20<=l<=21		-12<=h<=14, -12<=k<=12, -24<=l<=23	
Reflections collected	11935		25529	
Independent reflections	3221 [R(int) = 0.0543]		4680 [R(int) = 0.0508]	
Completeness to theta = 24.999°	100.1 %		99.9 %	
Absorption correction	Semi-empirical from equivalents		Semi-empirical from equivalents	
Max. and min. transmission	0.995 and 0.990		0.995 and 0.991	
Refinement method	Full-matrix least-squares on F^2		Full-matrix least-squares on F^2	
Data / restraints / parameters	3221 / 1 / 223		4680 / 1 / 237	
Goodness-of-fit on F^2	1.006		1.038	
Final R indices [I>2sigma(I)]	R1 = 0.0449, wR2 = 0.1028		R1 = 0.0581, wR2 = 0.1381	
R indices (all data)	R1 = 0.0560, wR2 = 0.1087		R1 = 0.1081, wR2 = 0.1653	
Absolute structure parameter	0.0(10)		-0.2(7)	

Extinction coefficient	n/a	n/a
Largest diff. peak and hole (e.Å^{-3})	0.195 and -0.191	0.420 and -0.228

3e. ORTEP diagram of polymorph II of tripeptide 1

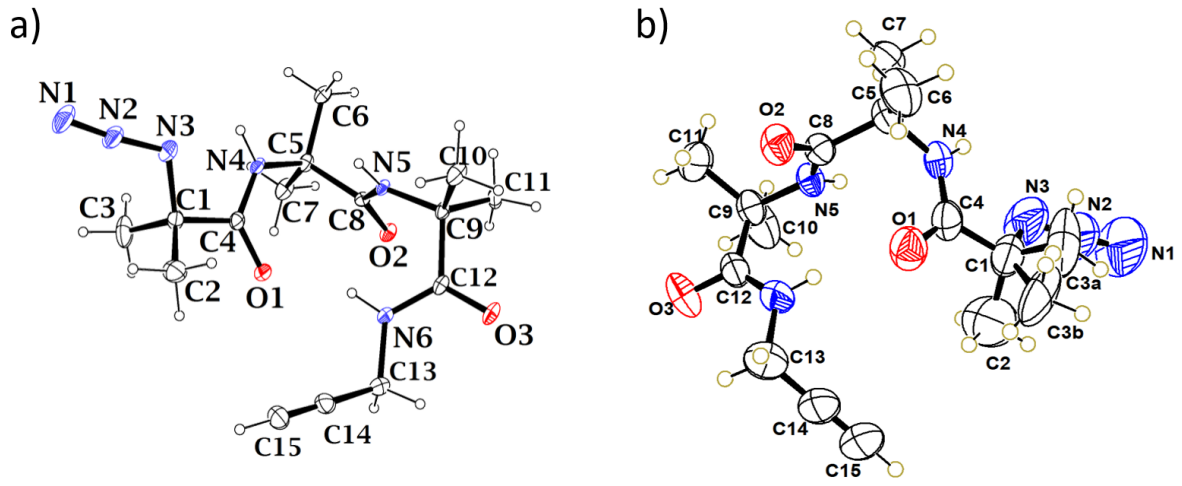

Fig. S2. ORTEP diagrams of polymorph **II** of tripeptide **1** determined at a) 150 K and b) 296 K (drawn with 50 % probability of ellipsoids).

3f. Non-covalent interactions present in polymorphs II

Table S4:

Type of interaction	D-H···A or N···O	Distance (H...A) (Å)
N-H···O	N5-H5···O3	2.032
C-H···N	C13-H13B···N1	2.844
C-H···H-C	C3-H3B···C13-H13A	2.417
	C13-H13B···C2-H2B	2.388
	C10-H10C···H2A-C2	2.339
C-H···O	C11-H11B···O3	2.675
	C7-H7B···O2	2.768
	C6-H6C···O2	2.457
	C15-H15A···O2	2.422
C-H···C	C13-H13B···C2	2.925
	C6-H6A···C15	2.859

3g. Crystal structure data for hydrate III of tripeptide 1

Table S5:

CCDC No:	2208398	
Empirical formula	$C_{15}H_{26}N_6O_4$	
Formula weight	354.42	
Temperature (K)	296(2)	
Wavelength (Å)	0.71073	
Crystal system	Monoclinic	
Space group	*P*21/*c*	
Unit cell dimensions	a = 17.887(3) Å	α = 90°
	b = 8.7802(12) Å	β = 108.215(5)°
	c = 12.944(2) Å	γ = 90°
Volume ($Å^3$)	1930.9(5)	
Z	4	
Density (calculated) (mg/cm^3)	1.219	
Absorption coefficient (mm^{-1})	0.090	
F(000)	760	
Crystal size (mm^3)	0.105 x 0.095 x 0.055	
Theta range for data collection	2.611 to 25.000°.	
Index ranges	-21<=h<=21, -10<=k<=10, -15<=l<=15	
Reflections collected	34282	
Independent reflections	3411 [R(int) = 0.0612]	
Completeness to theta = 25.000°	99.9 %	
Absorption correction	Semi-empirical from equivalents	
Max. and min. transmission	0.995 and 0.991	
Refinement method	Full-matrix least-squares on F^2	
Data / restraints / parameters	3411 / 6 / 268	
Goodness-of-fit on F^2	1.029	
Final R indices [I>2sigma(I)]	R1 = 0.0500, wR2 = 0.1228	
R indices (all data)	R1 = 0.0789, wR2 = 0.1414	
Extinction coefficient	n/a	
Largest diff. peak and hole ($e.Å^{-3}$)	0.285 and -0.209	

3h. ORTEP diagram of hydrate III of tripeptide 1

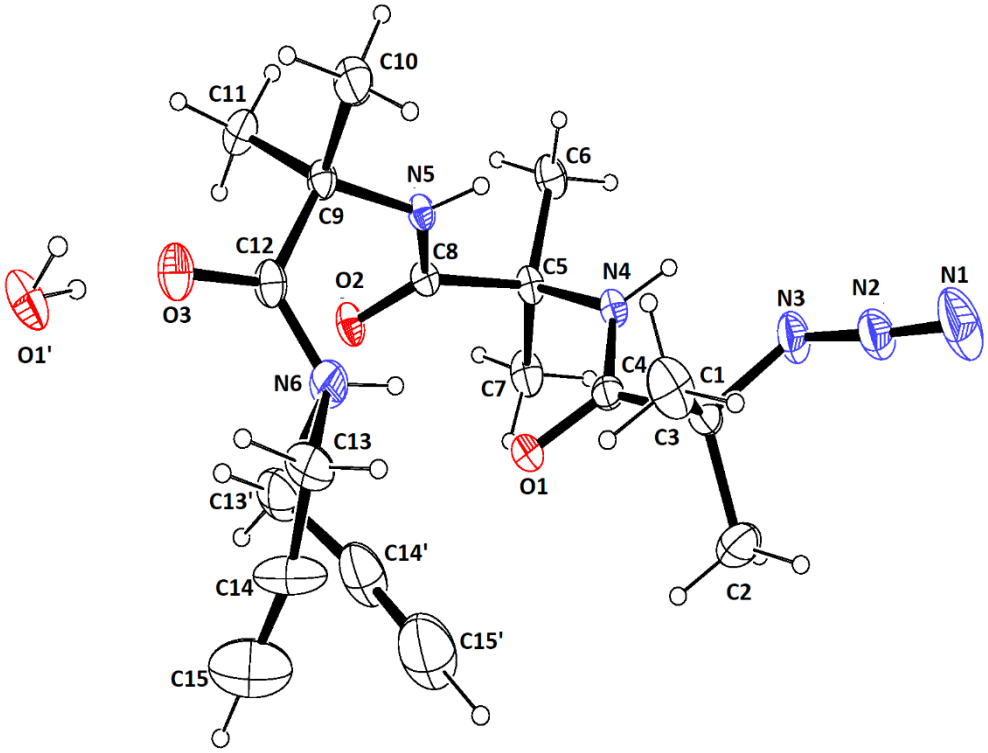

Fig. S3. ORTEP diagram of the hydrate **III** of tripeptide **1** drawn with 50 % probability of ellipsoids.

3i. Non-covalent interaction present in hydrate III

Table S6:

Type of interaction	D-H···A or N···O	Distance (H…A) (Å)
N-H···O	N5-H5···O1′	2.110
O-H···O	O1′H1B···O2	1.979
	O1′H1A···O3	1.969
N···O (Azide···oxygen)	N1···O1	3.028
	N2···O1	2.968
C-H···N	C7-H7C···N2	2.844
C-H···O	C11-H11A···O1′	2.810
C-H···C	C1-H1B···C7	2.948
	C15-H15···C15	2.605
C-H···H-C	C15-H15···H15-C15	2.297
	C13-H13A···H3C3	2.354
	C1-H1B···H7B-C7	2.402

Section S4. Phase purity analysis of all the polymorphic forms by PXRD

The crystals grown in each mixture of solvents were powdered and the PXRD pattern was recorded. This pattern was compared with the pattern simulated from the corresponding single-crystal structure.

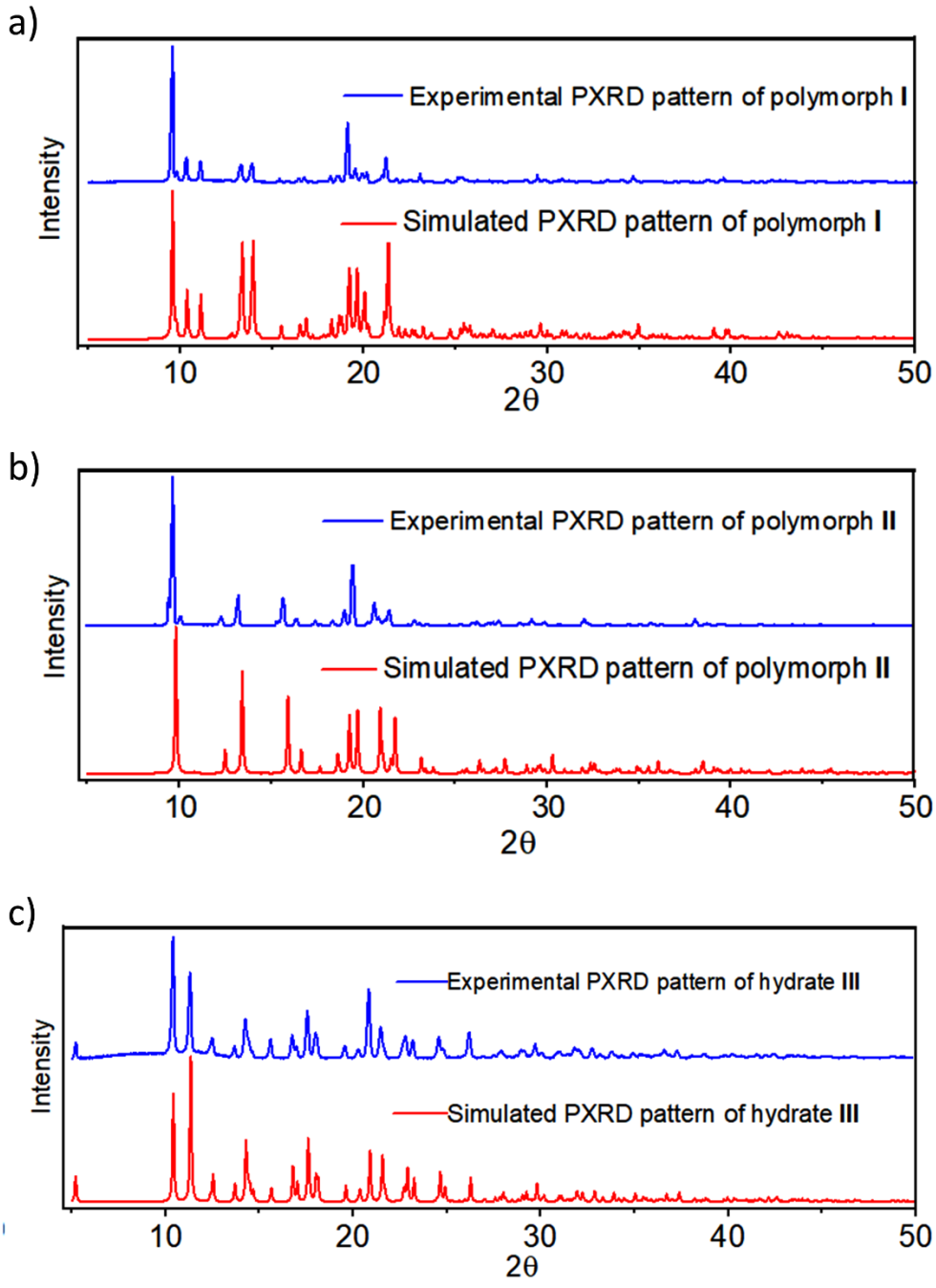

Fig. S4. Comparison of simulated and experimental PXRD pattern of monomer crystals of polymorphs a) **I**, b) **II**, and c) hydrate **III**, obtained in various solvents.

Section S5. Transition of hydrate III to polymorph II

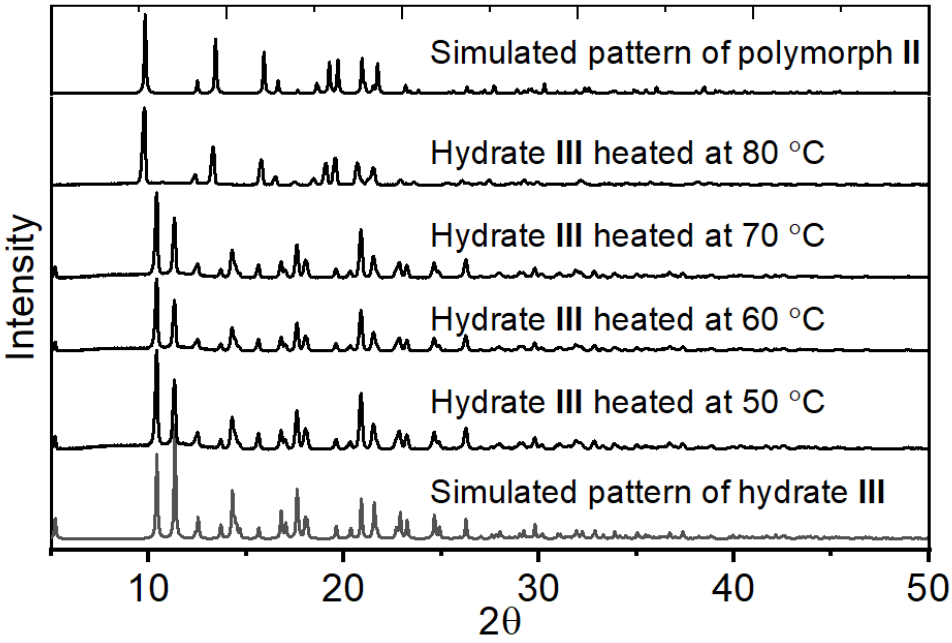

Fig. S5. Comparison of PXRD pattern of hydrate **III** after heating at 50 ºC, 60 ºC, 70 ºC and 80 ºC.

Section S6. Time-dependent studies during polymerization of tripeptide 1 at 80 ºC

Polymorphs **I** and **II** of tripeptide **1** were taken in separate glass vials and placed in an oil bath pre-heated at 80 ºC. Fractions from both samples taken at various intervals were analyzed using ^{1}H NMR spectroscopy.

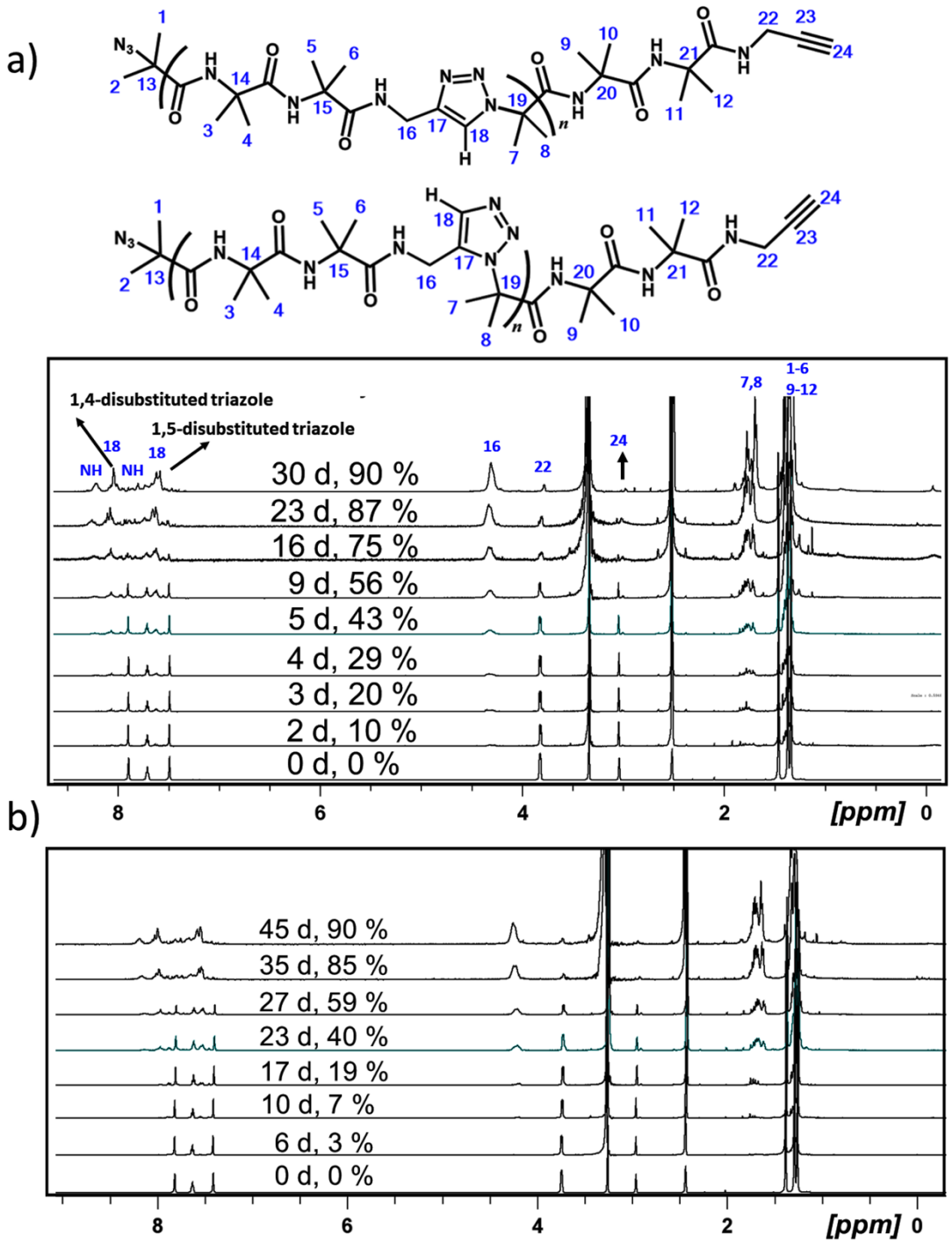

Fig. S6. Time-dependent ^{1}H NMR spectra (in DMSO-d_6) taken at various intervals of time during polymerization of polymorphs a) **I**, and b) **II** when heated at 80 °C.

Section S7. Assignment of protons corresponding to 1,4- and 1,5-triazole linkage in the ^{1}H spectrum of polymer

Although the triazolyl protons of both the regioisomers in the polymers merged with the peaks corresponding to amide protons in ^{1}H NMR spectrum, we identified the position triazolyl protons in the spectrum using HMQC. NOESY spectrum of polymer indicated the spatial interaction of H-15 at 7.63 ppm with H-13 but not with H-2 and H-3. Thus, this proton is assigned corresponding to 1,5- triazole linkage. H-15 at 8.08 ppm

showed spatial interaction with H-2, H-3 and H-13, thus it is assigned corresponding to 1,4-triazole linkage (Fig. S7).

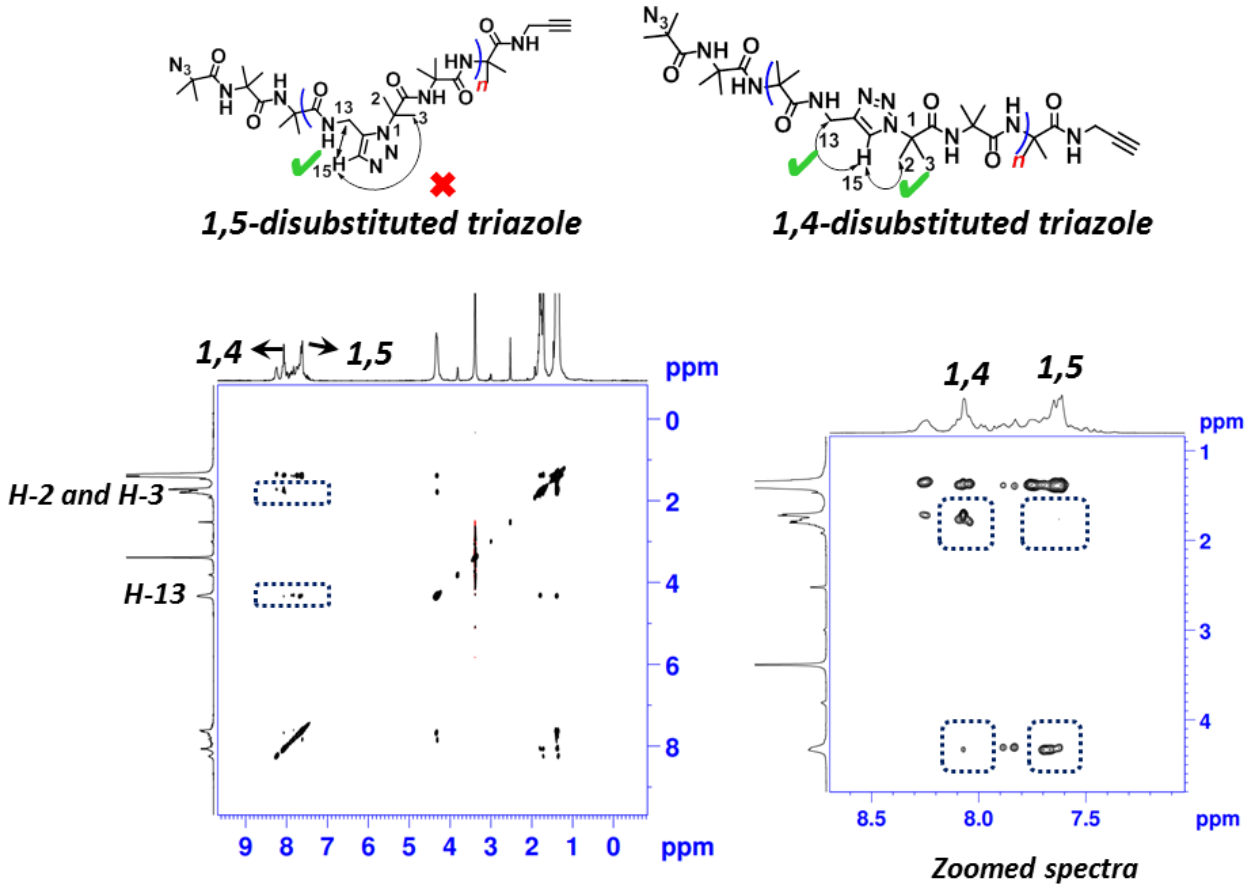

Fig. S7. NOESY spectrum of polymer of tripeptide **1** in polymorph **I** recorded in DMSO-d_6. Proton corresponding to 1,4- and 1,5- triazole linkage are assigned.

Section S8. Gel Permeation Chromatography (GPC) analysis

The polymer of tripeptide **1** in polymorphs **I** and **II** was dissolved in DMF (concentration 5 mg/mL). GPC analysis of this solution at 50 °C provided the following parameters. Polymethylmethacrylate (PMMA) calibration kits supplied by Agilent was used for column calibration.

Parameters	**Polymer of Polymorph I**	**Polymer of Polymorph II**
Mp (g/mol)	17940	10728
Mn (g/mol)	5174	4576
Mw (g/mol)	13975	11011
PDI	2.701	2.406

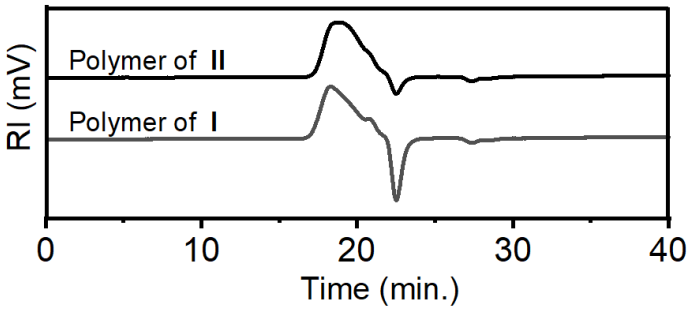

Fig. S8. Gel Permeation Chromatogram of polymer of polymorphs **I** and **II**.

Section S9. Comparison of polarising optical microscope images before and after polymerization of polymorphs I and II.

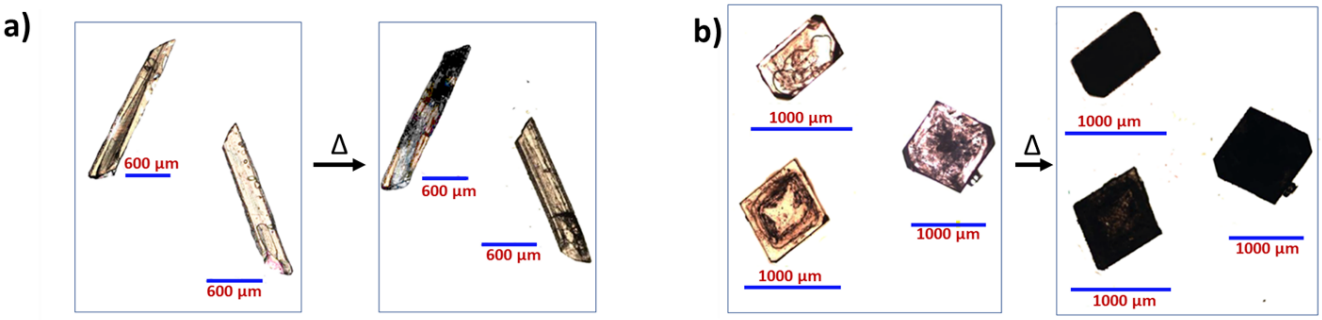

Fig. S9. Comparison of polarizing optical microscope images of polymorphs a) **I** and b) **II**; before and after polymerization

Section S10. Comparison of FTIR spectra of fresh and aged polymers of polymorph II

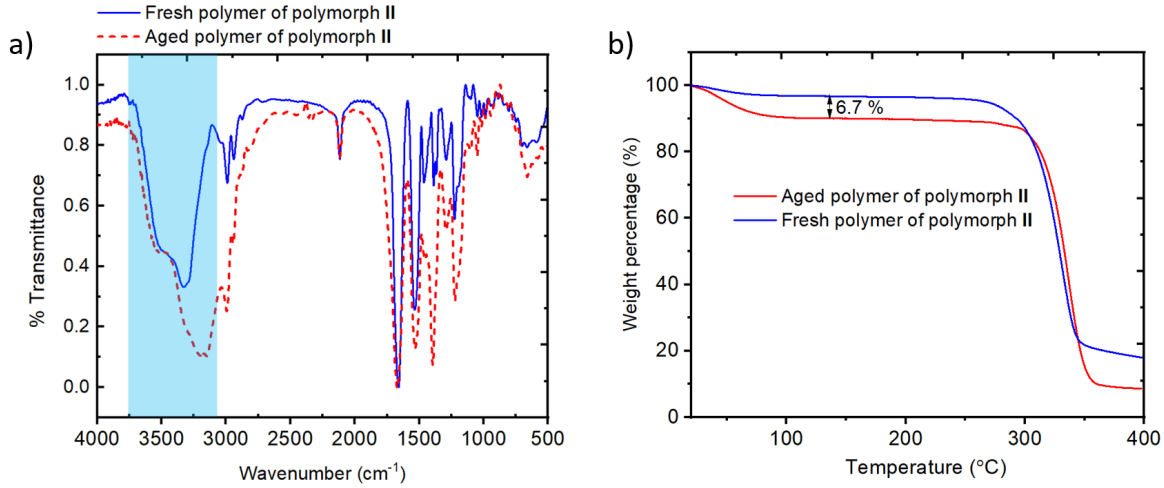

Fig. S10. a) Normalized FTIR spectra of aged and freshly polymerized polymer of polymorph **II**. The region in the spectra having the peak corresponding to OH-stretching of water has been highlighted in cyan. b) Comparison of TGA profiles of aged and freshly polymerized polymer of polymorph **II**.

Section S11. 11a) Crystal data for the polymer of polymorph I

Table S7:

CCDC No.	2208397	
Empirical formula	$C_{15}\ H_{24}\ N_6\ O_3$	
Formula weight	336.4	
Temperature (K)	296(2)	
Wavelength (Å)	0.71073	
Crystal system	Orthorhombic	
Space group	*Pbca*	
Unit cell dimensions	a = 17.885(5) Å	α= 90°
	b = 18.470(5) Å	β= 90°
	c = 10.697(3) Å	γ = 90°
Volume ($Å^3$)	3533.7(17)	
Z	8	
Density calculated (g/cm^3)	1.265	
Absorption coefficient (mm^{-1})	0.091	
F(000)	1440	
Crystal size (mm^3)	0.110 x 0.075 x 0.035	
Theta range for data collection	2.205 to 24.999°.	
Index ranges	-21<=h<=21, -21<=k<=21, -12<=l<=12	
Reflections collected	39620	
Independent reflections	3109 [R(int) = 0.1690]	
Completeness to theta = 25.242°	99.9 %	
Absorption correction	Semi-empirical from equivalents	
Max. and min. transmission	0.95 and 0.92	
Refinement method	Full-matrix least-squares on F^2	
Data / restraints / parameters	3109 / 2247 / 653	
Goodness-of-fit on F^2	1.144	
Final R indices [I>2sigma(I)]	R1 = 0.1183, wR2 = 0.3016	
R indices (all data)	R1 = 0.2678, wR2 = 0.4135	
Extinction coefficient	0.021(5)	
Largest diff. peak and hole ($e.Å^{-3}$)	0.346 and -0.343	

11b. ORTEP diagram of components in the polymer of polymorph I

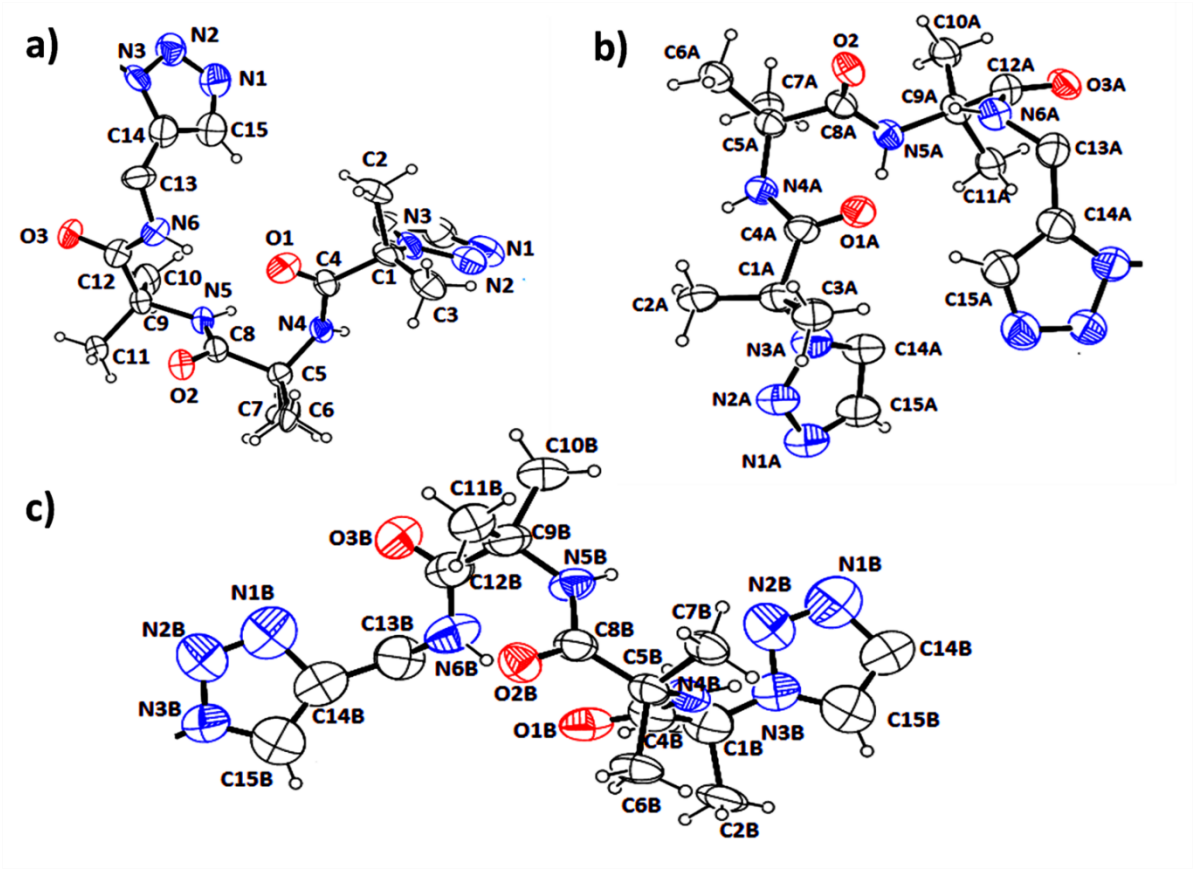

Fig. S11. ORTEP diagram of various components present in the crystal structure of polymer of polymorph **I** in the ratio (a) 0.432: (b) 0.077: (c) 0.491.

11c. Comparison of experimental PXRD pattern of polymer of polymorph I and simulated pattern obtained from the single-crystal diffraction data

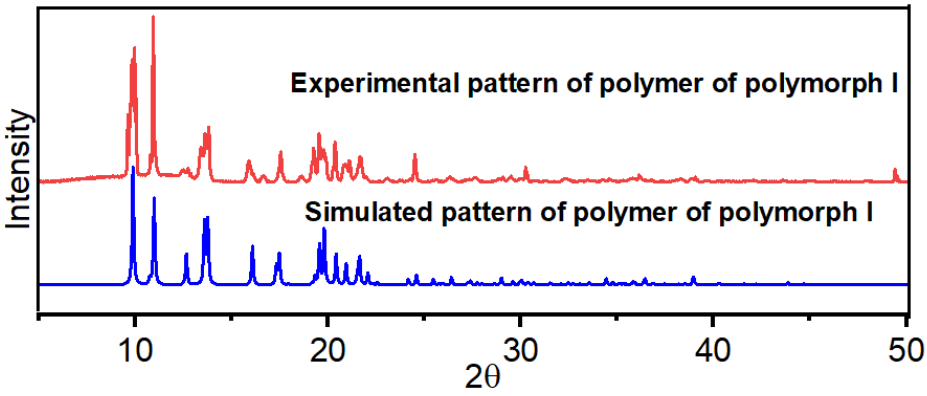

Fig. S12. Comparison of the simulated and experimental PXRD pattern of polymer of polymorph **I**.

Section S12. Time-dependent ^{13}C spectrum recorded during the polymerization of polymorphs I and II.

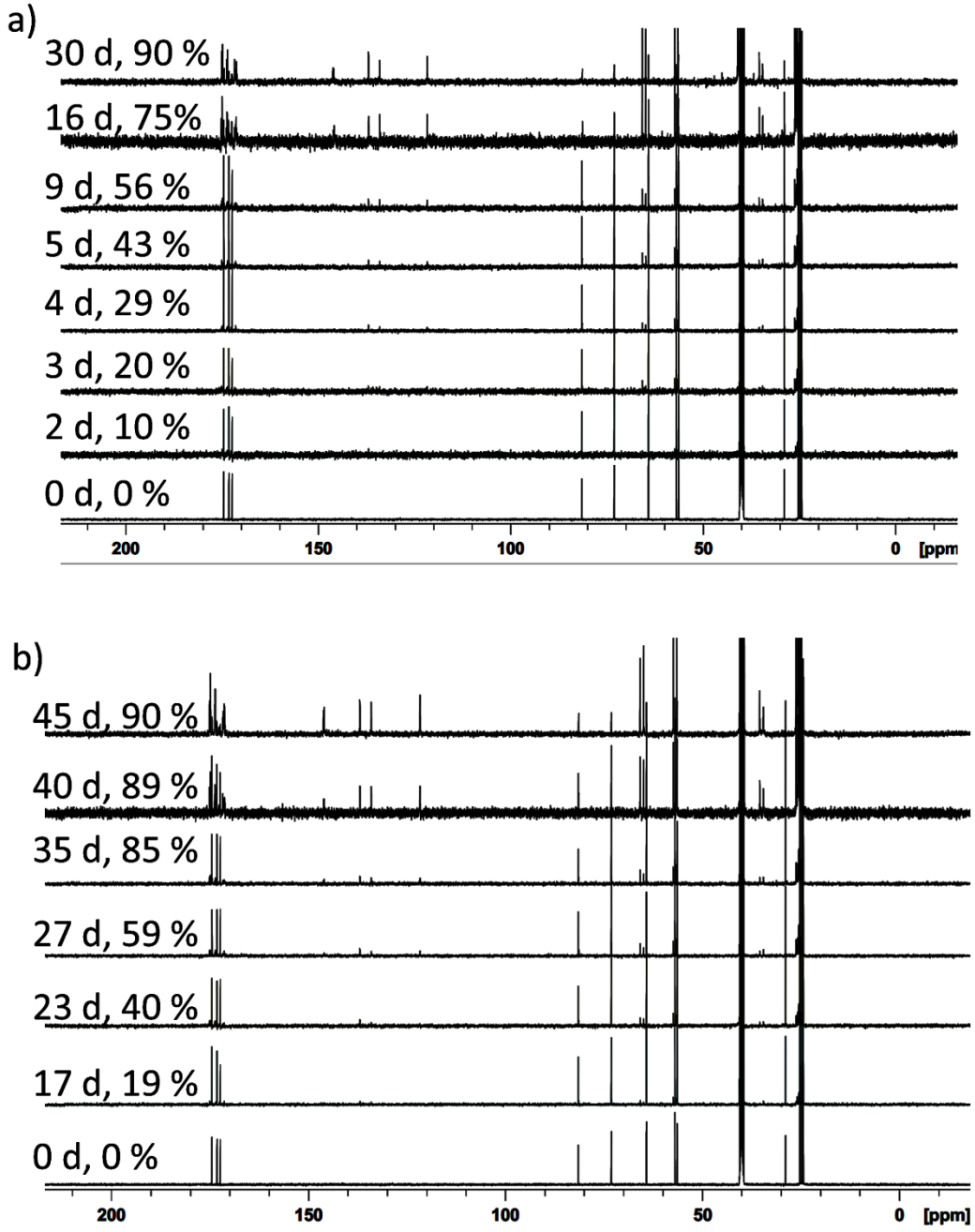

Fig. S13. Time dependent ^{13}C NMR recorded during the polymerization of polymorphs a) **I** and b) **II**, showing the peaks corresponding to both the 1,4- and 1,5-triazole linkages (at 121.7 ppm and 134 ppm, respectively).

Section S13. Plausible rotation of bonds connecting azide and alkyne during polymerization resulting in 1,4 and 1,5-triazole linkages

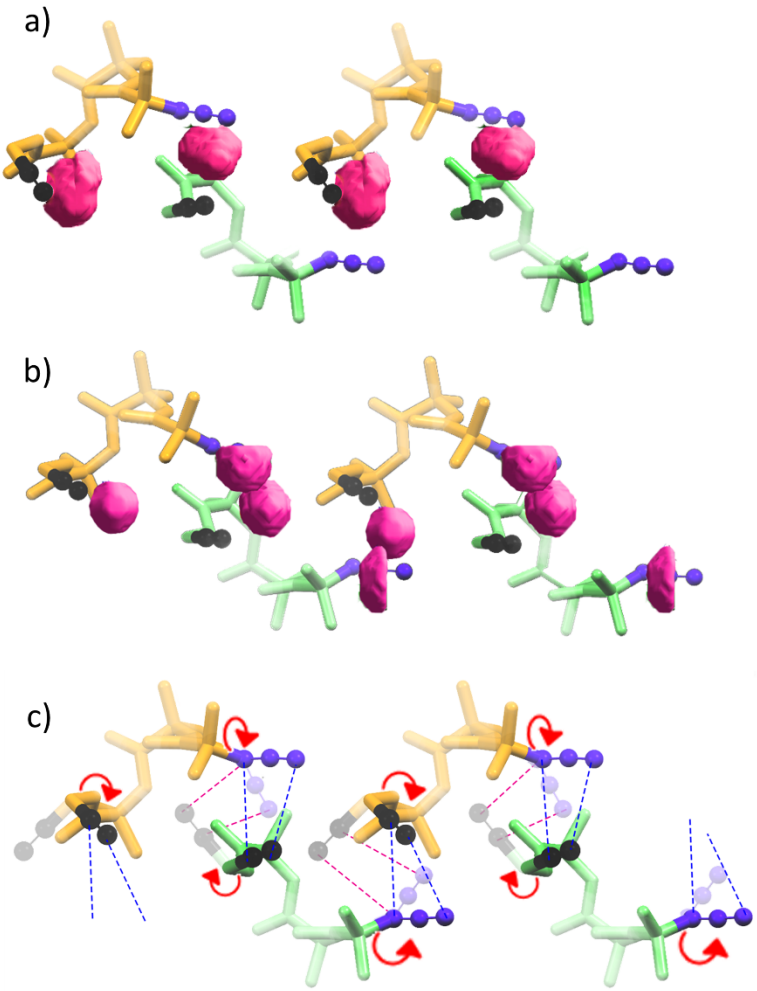

Fig. S14. Voids at the vicinity of azide and alkyne observed for a) polymorph **I** and b) **II** (voids at the vicinity of azide and alkyne are only shown for clarity, probe radius = 0.9 Å). c) Rotation of bonds connecting azide and alkyne to the peptide backbone of polymorphs **I** or **II** to obtain an arrangement suitable for formation of a 1,4-triazole linkage upon cycloaddition between the molecules of opposite helicity. Since relative arrangement of molecules in both the polymorphs **I** and **II** are the same, the rotation is shown only for polymorph **I**. Structure obtained after rotation is shown in faded color. Direction of rotation is shown in red-colored arrows.

Section S14. FT-IR spectra of monomer and polymer of polymorphs I and II

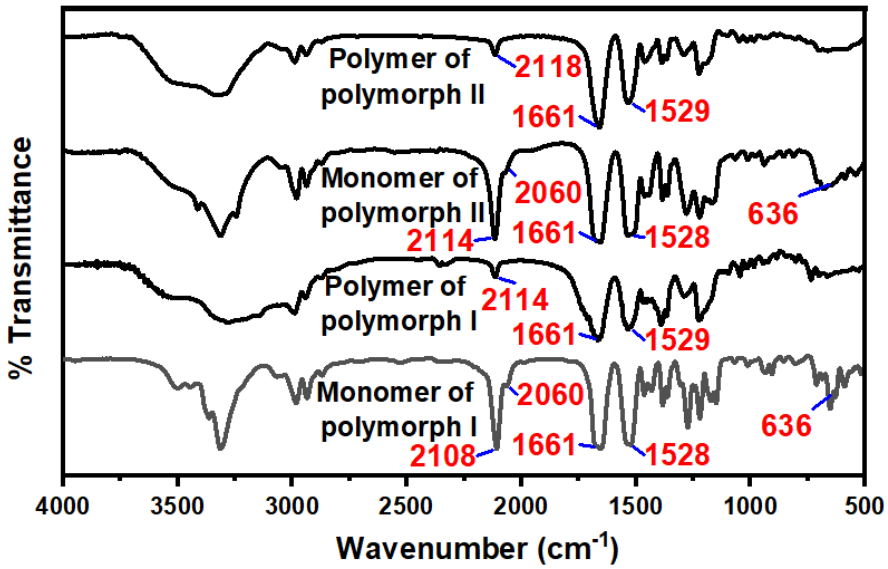

Fig. S15. Comparison of FT-IR spectra of monomer and polymer of polymorphs **I** and **II**. Amide I and II peaks (1661 cm^{-1} and 1528 cm^{-1} respectively) characteristic of a β-turn peptide are retained even after polymerization. The signals due to azide (2108-2118 cm^{-1}) and alkyne (2060 cm^{-1} and 636 cm^{-1}) are diminished in the polymer samples as they are consumed during polymerization.

Section S15. Comparison of PXRD of polymers of polymorphs I and II

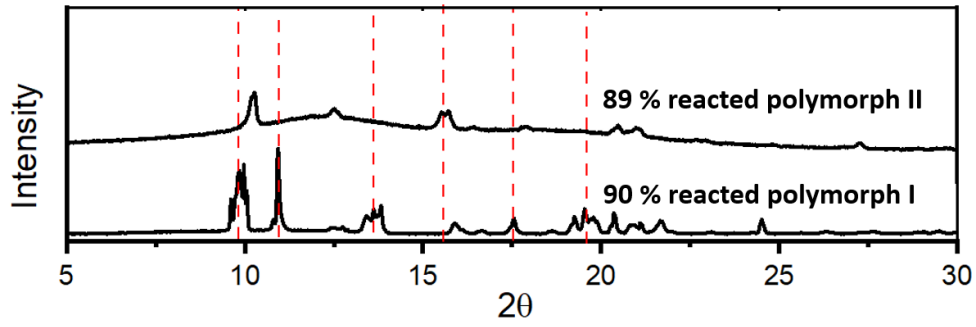

Fig. S16. Comparison of PXRD patterns of completely reacted polymorph **I** (90%) and polymorph **II** (89%) showing difference in the packing.

Section S16. Comparison of solid-state ^{13}C CP/MAS NMR spectra of polymers of polymorphs I and II

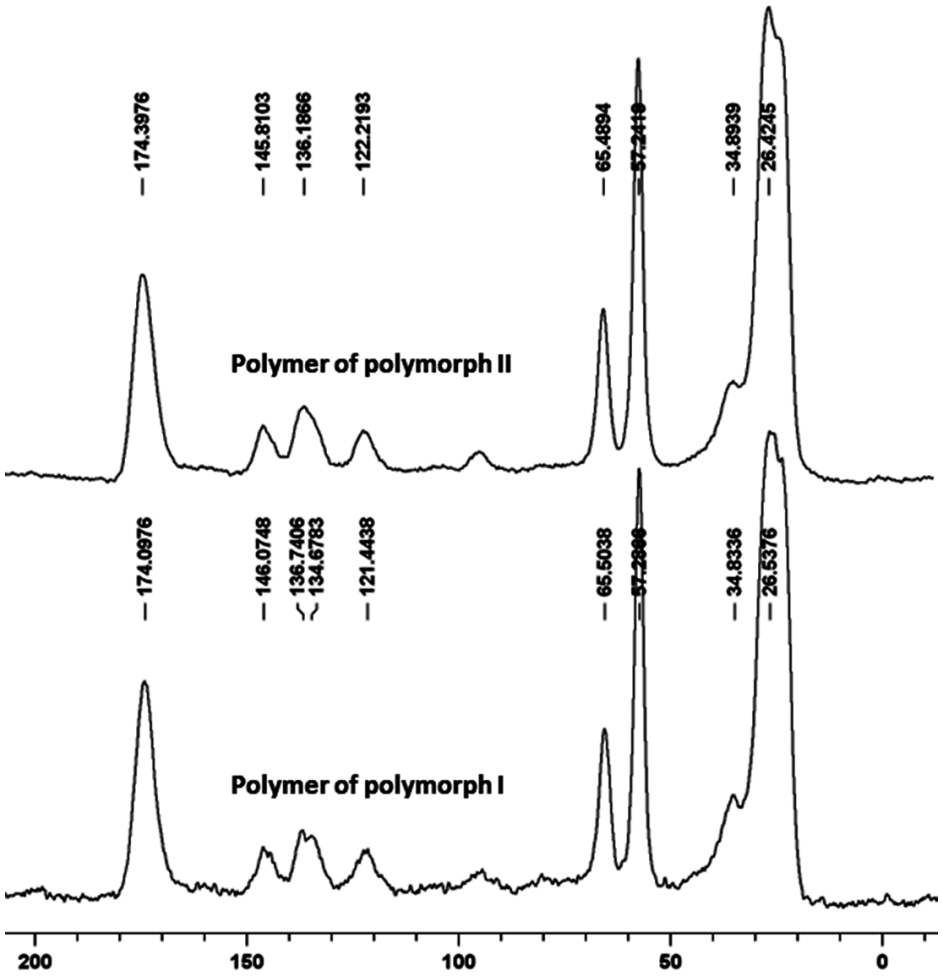

Fig. S17. Solid-state ^{13}C CP/MAS NMR spectra of polymers of polymorphs **I** and **II** showing negligible changes in the δ values.

Section S17. Thermo-Gravimetric Analysis (TGA) of polymer of polymorphs I, and II

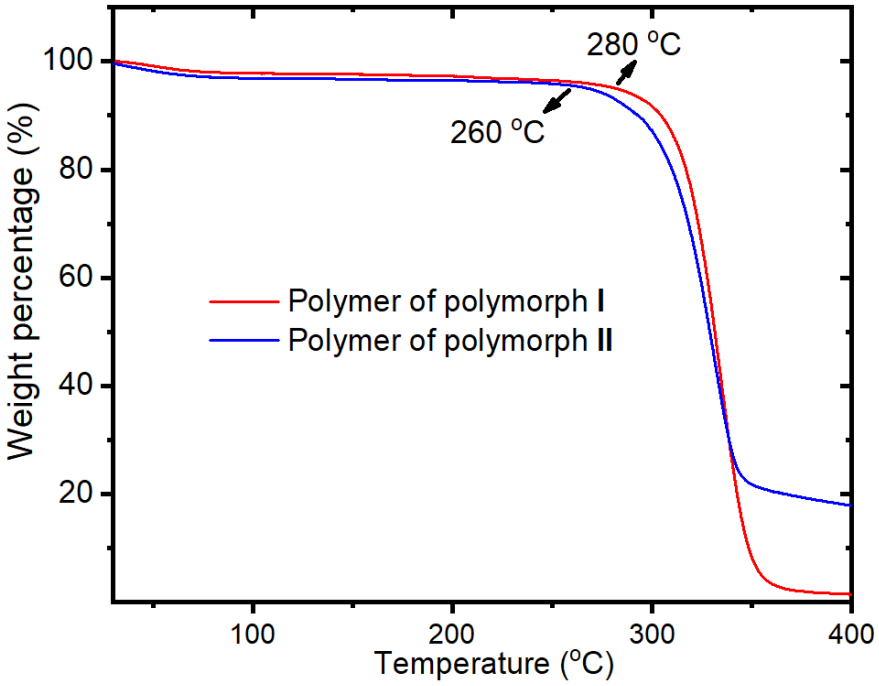

Fig. S18. Thermo-Gravimetric Analysis of polymer of polymorphs **I** and **II**, showing the thermal stabilities up to 280 °C and 260 °C, respectively. The decrease in weight at ~75 °C could be due to the evaporation of moisture trapped by the polymers.

Section S18. DSC profiles of polymers of polymorphs I and II

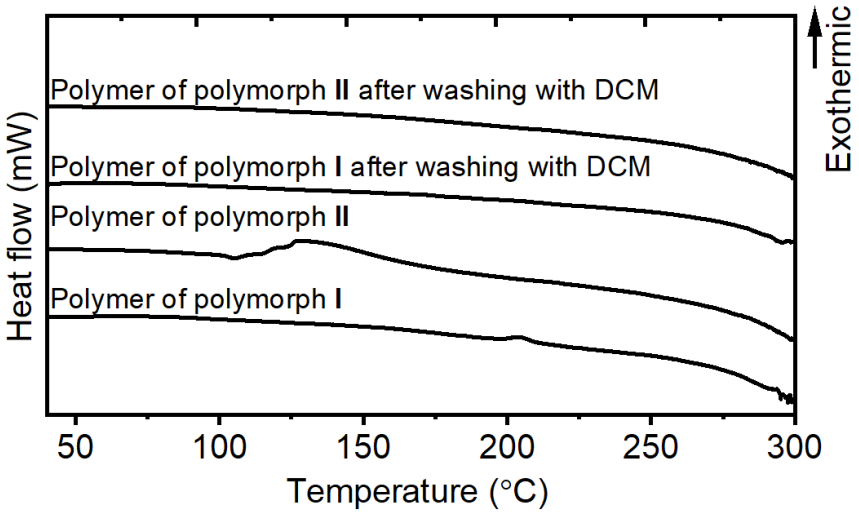

Fig. S19. DSC profiles recorded at a heating rate of 1 °C/min. for the crude polymer of polymorphs **I** and **II**; and polymers washed with DCM. The negligible exothermic peak at 204 °C in the DSC profile of the polymer of polymorph **I** could be ascribable to the exothermic azide-alkyne cycloaddition of partially reacted oligomers occurring in their melt domains. This peak disappeared when the partially reacted oligomers were washed off using DCM.

Section S19. Nanoindentation

Prior to nanoindentation, we indexed the faces of crystals of the monomer of polymorphs **I**, **II**, and **III**. Some of the crystals were heated for polymerization, by placing the face required for indentation exposed above a glass slide. We carried out the face indexing of single crystals using 'Bruker AXS Face-indexing User Interface', from a Bruker KAPPA APEX-II diffractometer in omega and phi scan mode. The crystals were glued on a magnetic stub using cyanoacrylate glue.

We performed nanoindentation using a nanoindenter (Hysitron Triboindenter (TI980), Minneapolis, USA) which is capable of atomic force microscopy (AFM) imaging. We used a three-sided pyramidal Berkovich diamond indenter with Poisson's ratio = 0.07. We applied a maximum load of 1 mN with loading and unloading indentation speed of 0.1 mN s^{-1}. At the maximum peak load of 1 mN, the tip was held for 10 s. We performed 15-20 indentations on each face and the average of the most reproducible values is reported. The elastic modulus (E) and indentation hardness (H) were estimated using the Oliver–Pharr method.[6] The reduced modulus (E_r) was obtained from the load-displacement (P-h) curves using the following equation.

$$\text{Reduced modulus, } E_r = \frac{\sqrt{\pi}}{2\beta}\frac{S}{\sqrt{A_c}}$$

where 'S' is the contact stiffness, 'A_c' is the contact area under load and 'β' is a constant that depends on the geometry of the indenter. 'S' is the slope of the P-h curves at the initial point of unload ($S = dP/dh$). For Berkovich tip β = 1.034. The reduced modulus 'E_r ' was converted into elastic modulus (Young's modulus, E) using the equation:

$$\frac{1}{E_r} = \frac{1-\upsilon_i^2}{E_i} + \frac{1-\upsilon_s^2}{E_s}$$

where 'E_i' and 'E_s ' are the elastic moduli of the indenter and the sample respectively, 'υ_i' and 'υ_s ' are the Poisson's ratio of the indenter and the sample respectively. For the indenter used 'E_i' = 1141 GPa and 'υ_i' = 0.07. 'υ_s' for all the crystals were taken as 0.3.

The hardness (H) is the ratio of maximum indentation load (P_{max}) to the contact area (A_c):

$$H = \frac{P_{max}}{A}$$

Contact area (A_c) was calibrated as a function of contact depth (h_c) as $\boldsymbol{A_c} = f(h_c)$. The contact depth '$h_c$' is obtained from the load-displacement plot:

$$\boldsymbol{h_c} = \boldsymbol{h_{max}} - \boldsymbol{\varepsilon}\frac{P_{max}}{S}$$

where h_{max} is the maximum indentation depth and $\boldsymbol{\varepsilon}$ = 0.75 for Berkovich tip.

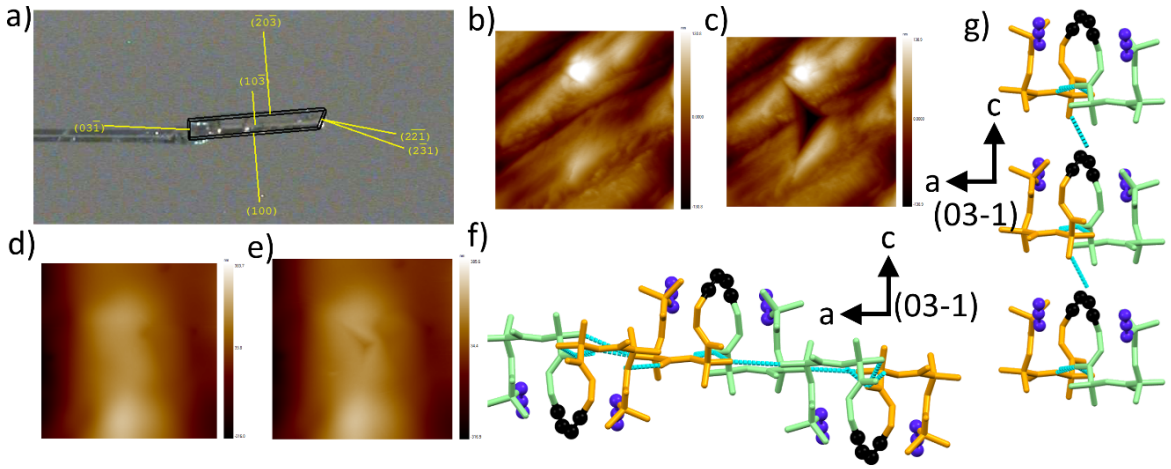

Fig. S20. a) Face indexing done on monomer-crystals of polymorph **I**. b,c) Scanning probe images of surfaces of the monomer crystals of polymorph **I** (b) before and (c) after indentation. d,e) Scanning probe images of surfaces of polymer crystals of polymorph **I** (d) before and (e) after indentation. f,g) Non-covalent interactions between the tripeptide molecules along (f) a-axis and (g) c-axis. The interactions are shown in cyan dotted lines and are tabulated in table S8.

Table S8: Non-covalent interactions present in the 'ac' plane (plane perpendicular to direction of indentation, (03-1) plane) in polymorph **I**

Type of non-covalent interaction		**D-H···A**	**Distance (H···A) (Å)**
Along 'a'- axis	N-H···O	N4A-H4A···O2A	2.64
	C-H···C	C10B-H10E···C6A	2.88
Along 'c' -axis	C-H···HC	C15A-H15A···H10F-C10B	2.39
	C-H···C	C11A-H11A···C15A	2.89
Along direction of indentation (b-axis)	N-H···O	N5A-H5A···O3B	2.098
		N5B-H5B···O3A	2.271
	C-H···O	C10B-H10E···O3A	2.429

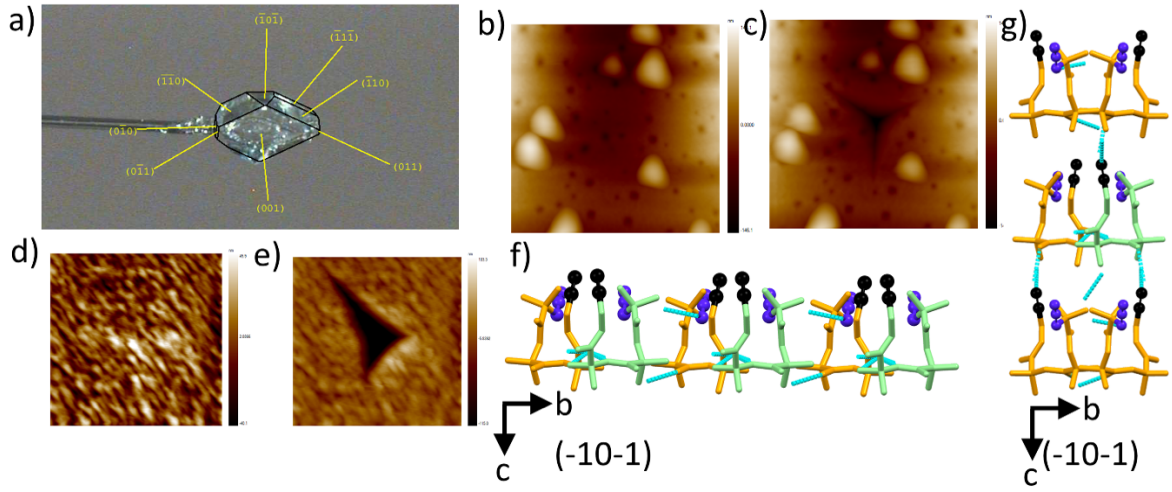

Fig. S21. a) Face indexing done on monomer-crystals of polymorph **II**. b,c) Scanning probe images of surfaces of the monomer crystals of polymorph **II** (b) before and (c) after indentation. d,e) Scanning probe images of surfaces of polymer crystals of polymorph **II** (d) before and (e) after indentation. f,g) Non-covalent interactions between the tripeptide molecules along (f) b-axis and (g) c-axis. The interactions are shown in cyan dotted lines and are tabulated in table S9.

Table S9: Non-covalent interactions present in the 'bc' plane (plane perpendicular to the direction of indentation, (-10-1) plane) in polymorph **II**

Type of non-covalent interaction		**D-H···A**	**Distance (H···A) (Å)**
Along 'b' -axis	C-H···HC	C13-H13B···C2-H2B	2.39
	C-H···O	C6-H6C···O2	2.457
Along 'c'- axis	C-H···O	C15-H15A···O2	2.422
	C-H···C	C6-H6A···C15	2.859
	C-H···H-C	C10-H10C···H2A-C2	2.339
Along direction of indentation (a-axis)	N-H···O	N5-H5···O3	2.032
	C-H···O	C11-H11B···O3	2.768

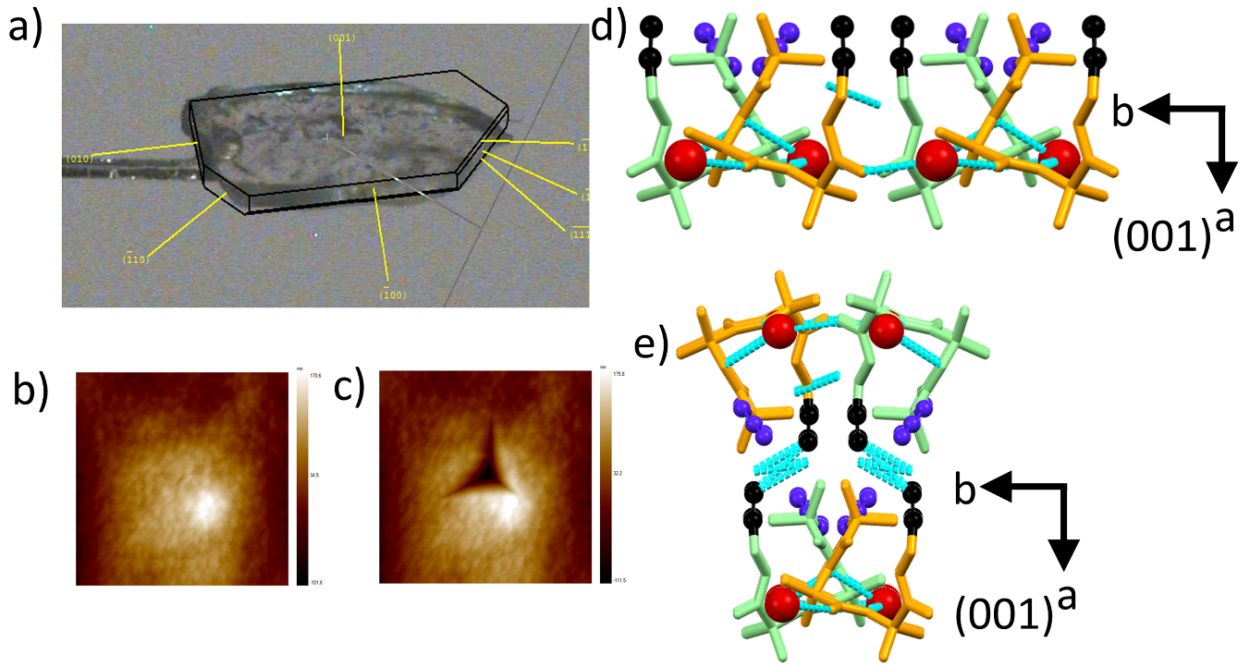

Fig. S22. a) Face indexing done on monomer-crystals of hydrate **III**. b,c) Scanning probe images of surfaces of the monomer crystals of hydrate **III** (b) before and (c) after indentation. d,e) Non-covalent interactions between the tripeptide molecules along (d) b-axis and (e) a-axis. The interactions are shown in cyan dotted lines and are tabulated in table S10.

Table S10: Non-covalent interactions present in the 'ab' plane (plane perpendicular to direction of indentation, (001) plane) in hydrate **III**

Type of non-covalent interaction		**D-H···A**	**Distance (H···A) (Å)**
Along 'a -axis	C-H..H-C	C15-H15···H15-C15	2.297
Along 'b- axis	O-H···O	O1'H1A···O3	1.969
	C-H···H-C	C13-H13A···C3-H3C	2.354
Along direction of indentation (c-axis)	N-H···O	N5-H5···O1'	2.110
	O-H···O	O1'H1B···O2	1.979

Section S20. NMR spectra

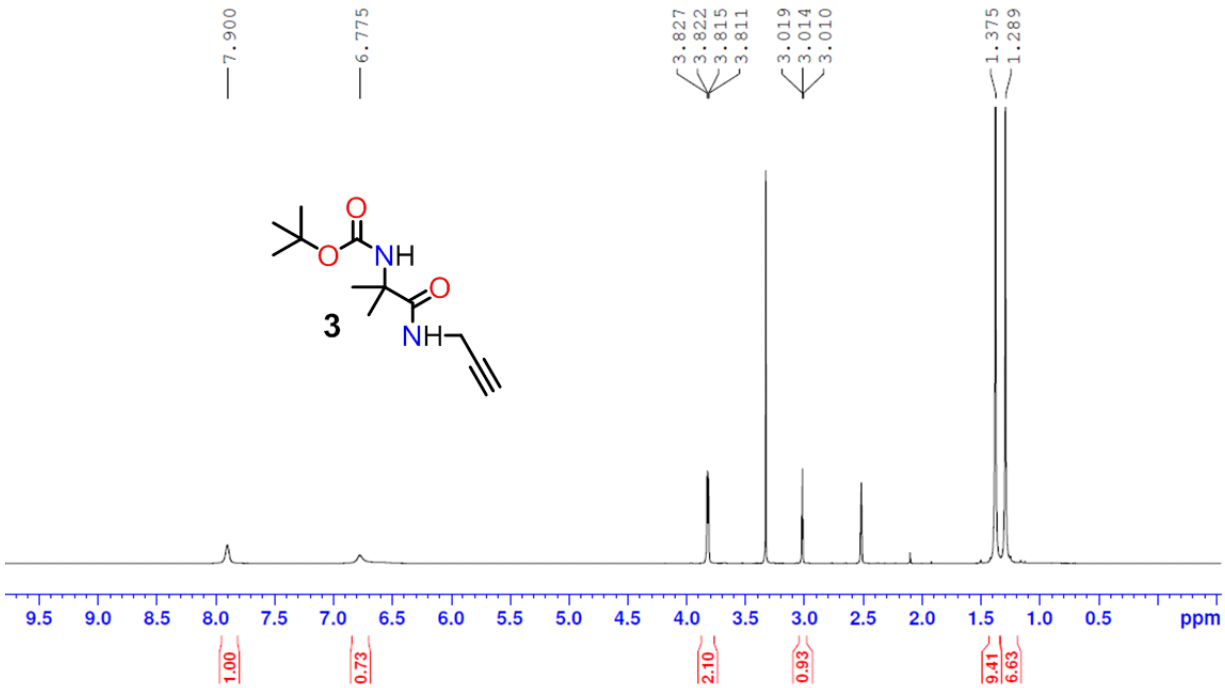

Fig. S23. ^{1}H NMR spectrum of compound **3** recorded in DMSO-d$_6$

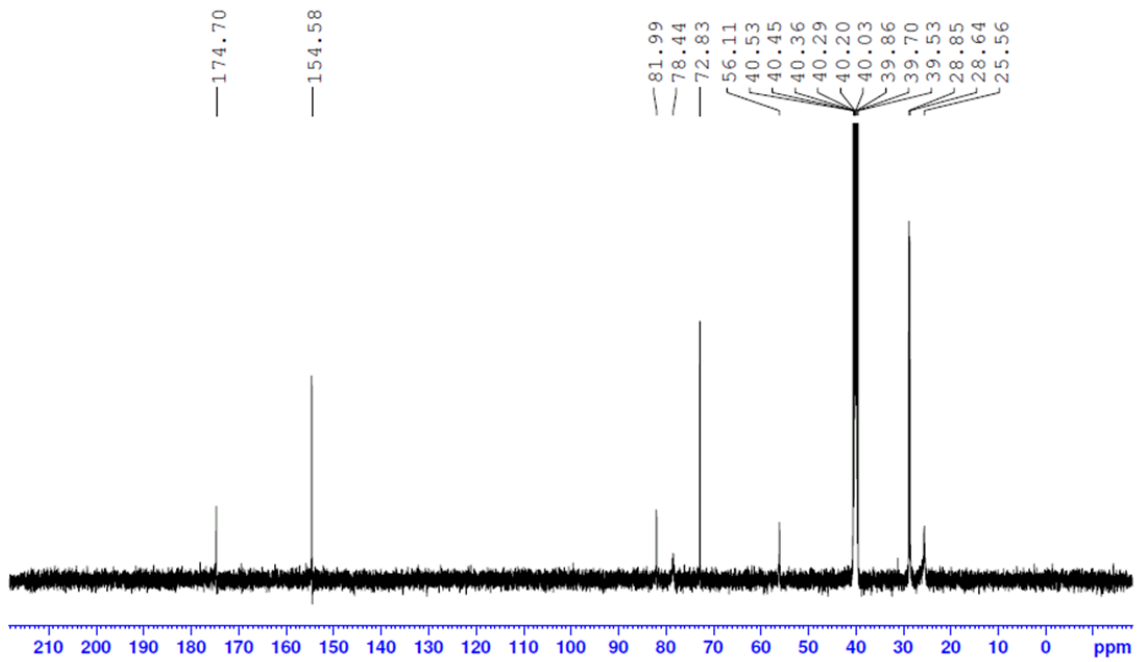

Fig. S24. ^{13}C spectrum of compound **3** recorded in DMSO-d$_6$

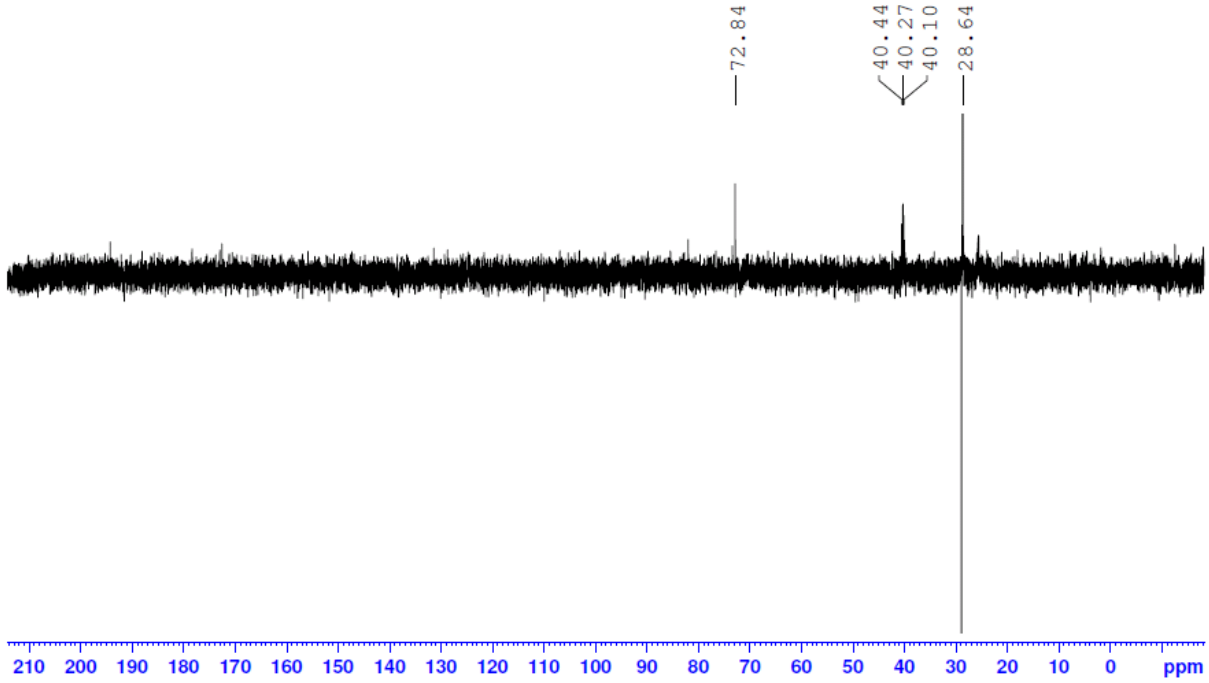

Fig. S25. DEPT spectrum of compound **3** recorded in DMSO-d_6

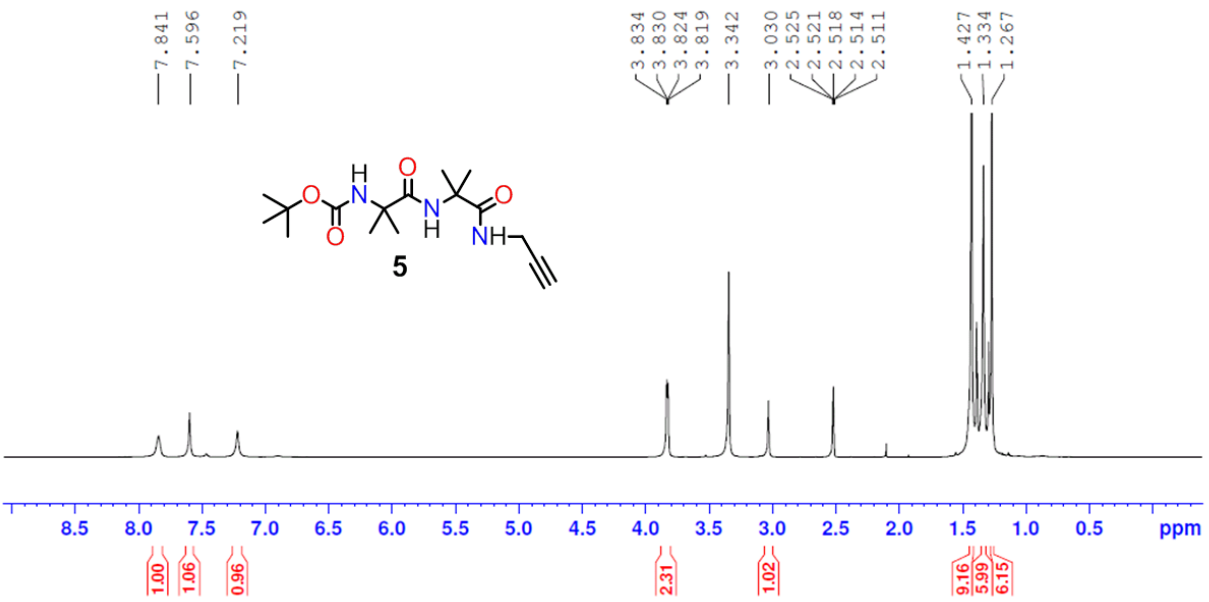

Fig. S26. ^{1}H spectrum of compound **5** recorded in DMSO-d_6

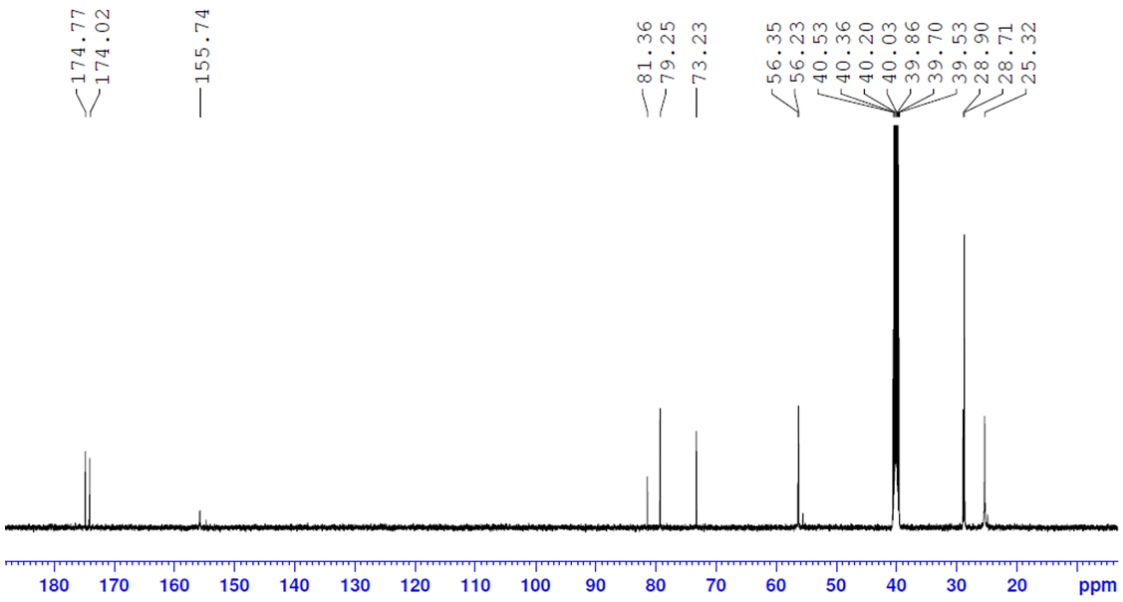

Fig. S27. ^{13}C spectrum of compound **5** recorded in DMSO-d_6

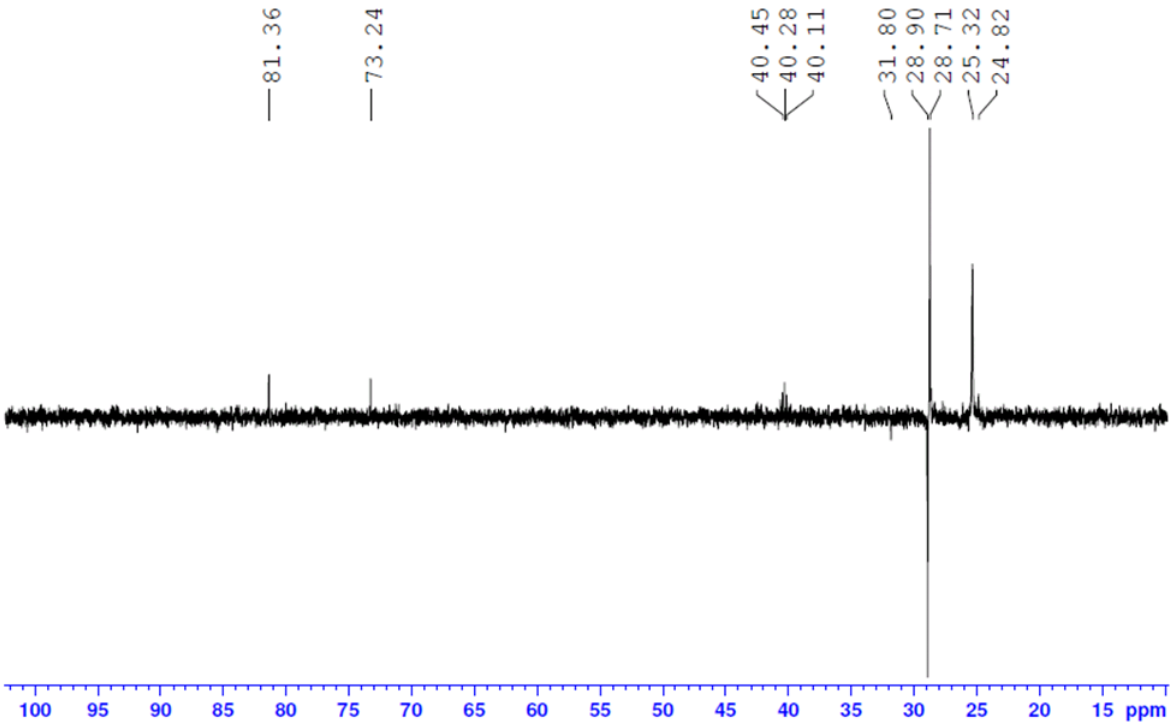

Fig. S28. DEPT spectrum of compound **5** recorded in DMSO-d_6

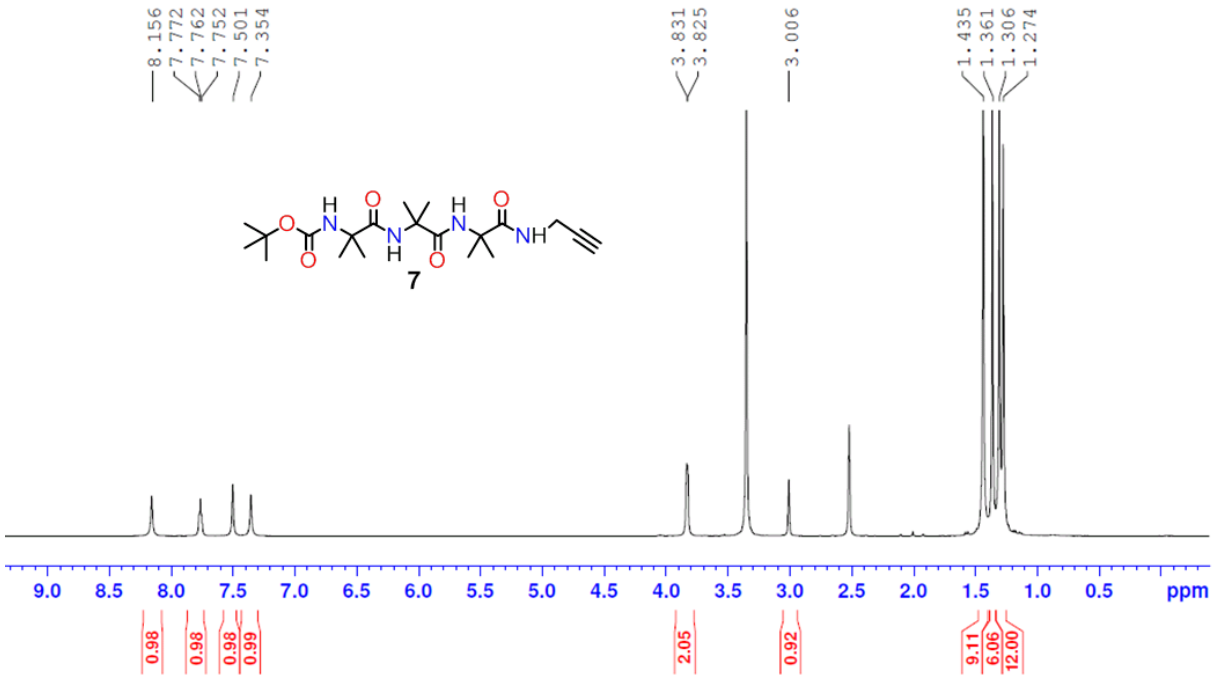

Fig. S29. ^{1}H spectrum of compound **7** recorded in DMSO-d_6

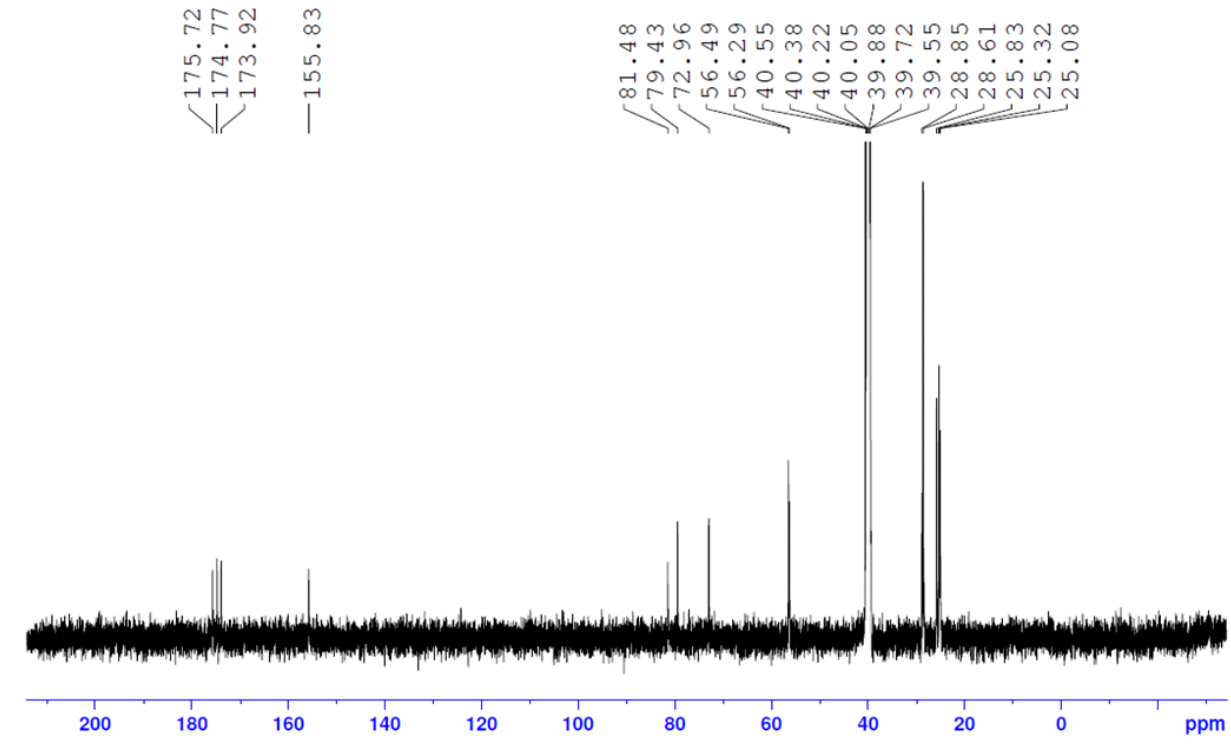

Fig. S30. ^{13}C spectrum of compound **7** recorded in DMSO-d_6

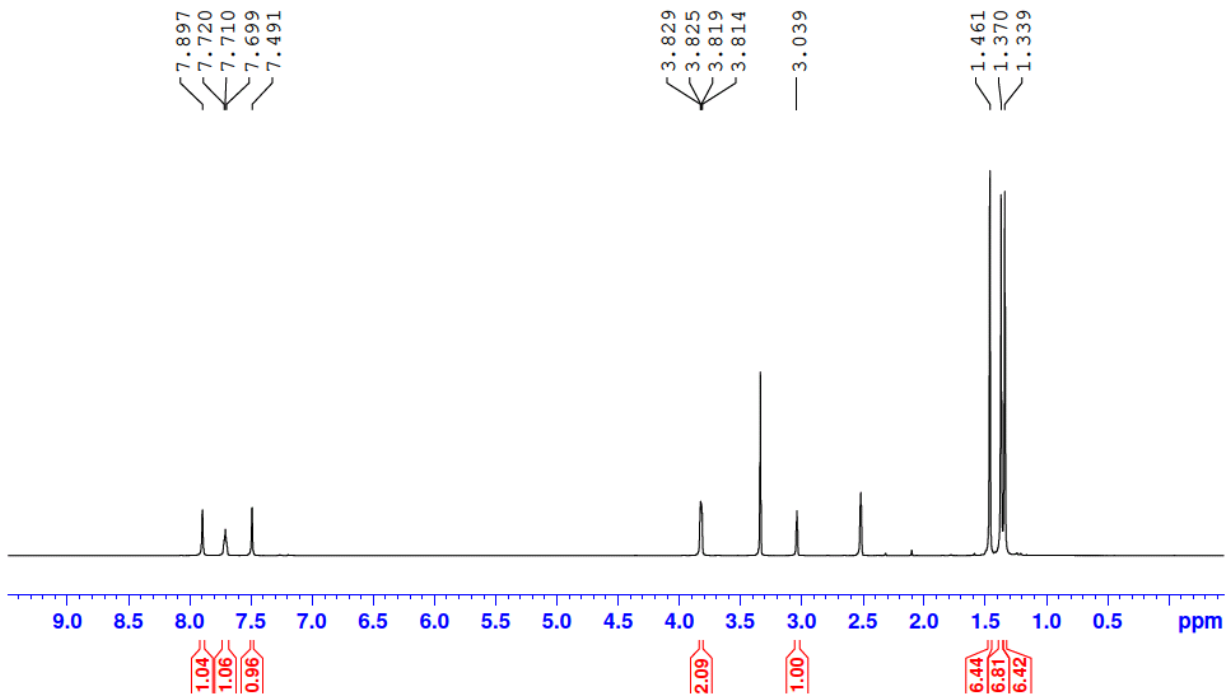

Fig. S31. [1]H NMR spectrum of tripeptide **1** recorded in DMSO-d6

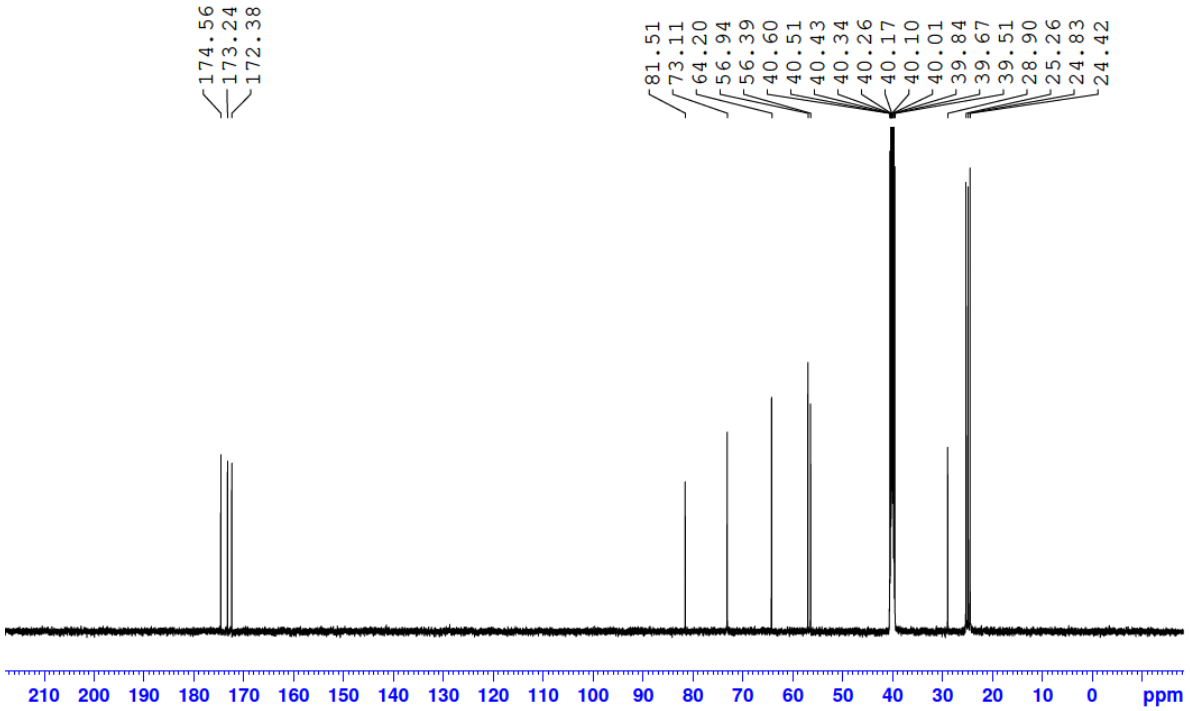

Fig. S32. [13]C spectrum of tripeptide **1** recorded in DMSO-d6

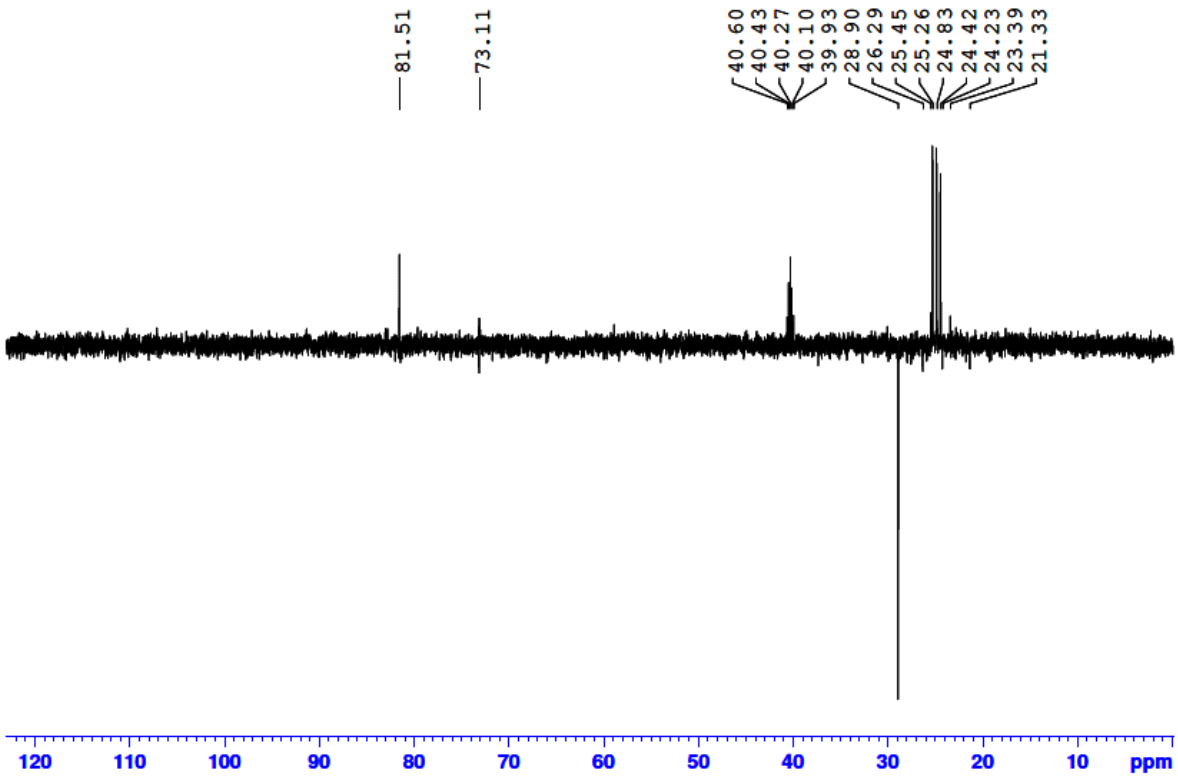

Fig. S33. DEPT spectrum of tripeptide **1** recorded in DMSO-d_6

Section S21. References

1. G. M. Sheldrick, SADABS, *Program for Empirical Absorption Correction for Area Detector Data*, University of Gottingen, Gottingen, Germany, 1996.

2. Bruker, SAINT*, Data Reduction and Correction Program*, Bruker AXS, Madison, Wisconsin, USA, 2012.

3. G. M. Sheldrick, *Acta Crystallogr. Sect. A: Found. Crystallogr*., 2008, **D64**, 112-122.

4. G. M. Sheldrick, *Acta Crystallogr. Sect. A: Found. Crystallogr*., 2015, **C71**, 3-8.

5. C. F. Macrae, P. R. Edgington, P. McCabe, E. Pidcock, G. P. Shields, R. Taylor, M. Towler, J. van de Streek, *J. Appl. Cryst.,* 2006, **39**, 453-457.

6. W. C. Oliver, G. M. Pharr. *J. Mater. Res*., 1992, **7**, 1564-1583.